SAM transmethylation pathway and adenosine recycling to ATP are essential for systemic regulation and immune response

Pavla Nedbalova[1], Nikola Kaislerova[1], Lenka Chodakova[1], Martin Moos[2,3,#], Tomas Dolezal[1,#]

[1] Department of Molecular Biology and Genetics, Faculty of Science, University of South Bohemia, České Budějovice, Czech Republic

[2] Laboratory of Analytical Biochemistry and Metabolomics, Institute of Entomology, Biology Centre, Czech Academy of Sciences, České Budějovice, Czech Republic

[3] Department of Applied Chemistry, Faculty of Agriculture and Technology, University of South Bohemia, České Budějovice, Czech Republic,

Corresponding author - MM: moos@bclab.eu, TD: tomas.dolezal@prf.jcu.cz

ABSTRACT

During parasitoid wasp infection, activated immune cells of *Drosophila melanogaster* larvae release adenosine to conserve nutrients for immune response. S-adenosylmethionine (SAM) is a methyl group donor for most methylations in the cell and is synthesized from methionine and ATP. After methylation, SAM is converted to S-adenosylhomocysteine, which is further metabolized to adenosine and homocysteine. Here, we show that the SAM transmethylation pathway is up-regulated during immune cell activation and that the adenosine produced by this pathway in immune cells acts as a systemic signal to delay *Drosophila* larval development and ensure sufficient nutrient supply to the immune system. We further show that the up-regulation of the SAM transmethylation pathway and the efficiency of the immune response also depend on the recycling of adenosine back to ATP by adenosine kinase and adenylate kinase. We therefore hypothesize that adenosine may act as a sensitive sensor of the balance between cell activity, represented by the sum of methylation events in the cell, and nutrient supply. If the supply of nutrients is insufficient for a given activity, adenosine may not be effectively recycled back into ATP and may be pushed out of the cell to serve as a signal to demand more nutrients.

Keywords:

SAM transmethylation pathway, adenosine signaling, privileged immunity, Drosophila, S-adenosylhomocysteinase, adenosine kinase, adenylate kinase

INTRODUCTION

Upon activation, immune cells fundamentally change their metabolism, requiring an increased supply of nutrients, which is essential for their effective function. Additional nutrients are delivered to immune cells by redirecting metabolites away from other tissues, making the immune system metabolically privileged, or selfish within an organism. The concept of selfish immunity proposes insulin resistance as a mechanism by which activated immune cells ensure adequate nutrient supply (Straub 2014; Dolezal 2015; Krejčová et al. 2023). For example, we have recently shown that immune cells produce cytokines Upd2 and Upd3, which induce the production of the insulin signaling inhibitor Impl2 in muscle tissue via the Jak/Stat signaling pathway. Impl2 reduces the consumption of carbohydrates by muscle, making nutrients more available to immune cells (McMullen et al. 2024). Another mechanism by which immune cells gain privileged access to nutrients is through the release of adenosine. Extracellular adenosine signaling, through the adenosine receptor, reduces nutrient consumption by non-immune tissues and slows the development of the organism, again leaving more nutrients available for the immune system (Bajgar et al. 2015; Dolezal 2015; Bajgar and Dolezal 2018).

Adenosine signaling plays a variety of roles, especially in more complex organisms such as mammals. However, the release of adenosine as a signaling molecule from cells plays a universal role from the most primitive organisms, such as social bacteria, to humans (Newby 1984; Boison and Jarvis 2021). The release of adenosine is an indication of metabolic stress and signals to neighbouring cells to adjust their behaviour accordingly. For example, the bacterium *Myxococcus xanthus* responds to nutrient depletion by releasing adenosine, which initiates the aggregation of bacteria into fruiting bodies (Shimkets and Dworkin 1981). In mammals the heart muscles secrete adenosine during ischemia, which causes blood vessels to dilate to increase blood flow and delivery of oxygen and nutrients (Lloyd et al. 1988; Deussen 1989; Kroll, Deussen, and Sweet 1992; Reiss et al. 2019). Adenosine also plays an important role in the induction of sleep, torpor and hibernation, physiological states associated with energy conservation (Fredholm, Johansson, and Wang 2011; Boison and Jarvis 2021). Therefore, the use of extracellular adenosine by immune cells to suppress nutrient consumption in non-immune tissues, thereby conserving energy for the immune response, fits well with this evolutionarily conserved role of adenosine signaling.

Adenosine is produced intracellularly in two ways (Figure 1), by conversion from AMP by nucleotidases or in the S-adenosylmethionine (SAM) transmethylation pathway from S-adenosylhomocysteine (SAH) by S-adenosylhomocysteinase (Ahcy). The increase in AMP mainly reflects the lack of energy and metabolic stress. Cells use adenylate kinase to produce one ATP and one AMP from two ADP molecules. Increased AMP activates AMPK, which suppresses energy-consuming processes in the cell and activates energy-producing processes (Kloor and Osswald 2004; P. Dzeja and Terzic 2009). AMP is also converted by nucleotidases to adenosine, which is released from the cell via the equilibrative nucleoside transporter (ENT), where it signals the metabolic stress of the cell to surrounding cells and tissues via adenosine receptors (Dolezelova et al. 2007; Fenckova et al. 2011). This is typical of cells during ischemia when they are deprived of nutrients (Deussen 1989; Schädlich et al. 2023). Since activated AMPK suppresses the function of immune cells (Salminen, Hyttinen, and Kaarniranta 2011), we would expect that in the absence of nutrients and decreasing ATP levels, the accumulated AMP would be converted to adenosine and released from the cells, thus demanding a greater supply of nutrients.

In the SAM transmethylation pathway, ATP and methionine combine to produce SAM, which is the major methyl group donor for most methylations in the cell. The SAM transmethylation pathway is one of the largest consumers of ATP when the adenosyl moiety of ATP is incorporated into SAM (i.e., it is not a conversion of ATP to ADP as in energy transfer). After the methyl group is transferred to the target molecule by methyltransferase, SAM becomes SAH, which must be rapidly converted to homocysteine and adenosine, or it will block further methylation. As methylation increases in the cell, more SAM is formed and at the same time SAH is cleared more rapidly, leading to an increase in the SAM:SAH ratio, known as the methylation index. SAH is converted to homocysteine and adenosine by Ahcy, which works in both directions; for the "SAM to homocysteine + adenosine" direction to prevail, homocysteine and adenosine must also be metabolized or excreted from the cell very rapidly (Lu 2000; Kloor and Osswald 2004; Yu et al. 2019; Roy et al. 2020; Vizán, Di Croce, and Aranda 2021).

Homocysteine can either be recycled back to methionine, or further metabolized in the transsulfuration pathway (source of cysteine, H_2S, and antioxidants) (Sbodio, Snyder, and Paul 2019). Adenosine can be catabolized to inosine by adenosine deaminase (Novakova and Dolezal 2011), or recycled to AMP by adenosine kinase and further to ATP by adenylate kinase, glycolysis or oxidative phosphorylation (R. J. Zeleznikar et al. 1990; Robert J. Zeleznikar, Dzeja, and Goldberg 1995; P. P. Dzeja, Chung, and Terzic 2007; P. Dzeja and Terzic 2009). The importance of adenosine recycling to AMP by adenosine kinase is indicated by the dependence of the methylation cycle on the concomitant function of this enzyme (Lecoq et al. 2001; Bjursell et al. 2011; Moffatt et al. 2002). Since every single methylation in the cell is associated with the formation of one adenosine molecule, the amount of adenosine accurately reflects the intensity of the SAM transmethylation pathway. In a sense, it reflects the activity of the cell, because the more processes the cell has to activate, the more new molecules it has to methylate.

We have previously shown that activated immune cells preferentially acquire nutrients during immune response by releasing adenosine, subsequently reducing nutrient uptake in non-immune tissues, thereby leading to a delay in development (Bajgar et al. 2015; Bajgar and Dolezal 2018). To elucidate the origin of adenosine in activated immune cells, we investigated the role of the SAM transmethylation pathway. Given its upregulation and critical function in mammalian immune cells (Lawson et al. 2012; Yu et al. 2019; Roy et al. 2020), we hypothesized that this pathway is also a major source of adenosine in *Drosophila* immune cells. Our results confirm that the SAM transmethylation pathway is indeed upregulated in *Drosophila* hemocytes upon parasitoid wasp infection. In addition, we show that this pathway is not only essential for the immune response, but also a source of extracellular adenosine that slows larval development. Moreover, not all adenosine is released from hemocytes, but it can be recycled back into ATP and thus re-enter the SAM transmethylation pathway.

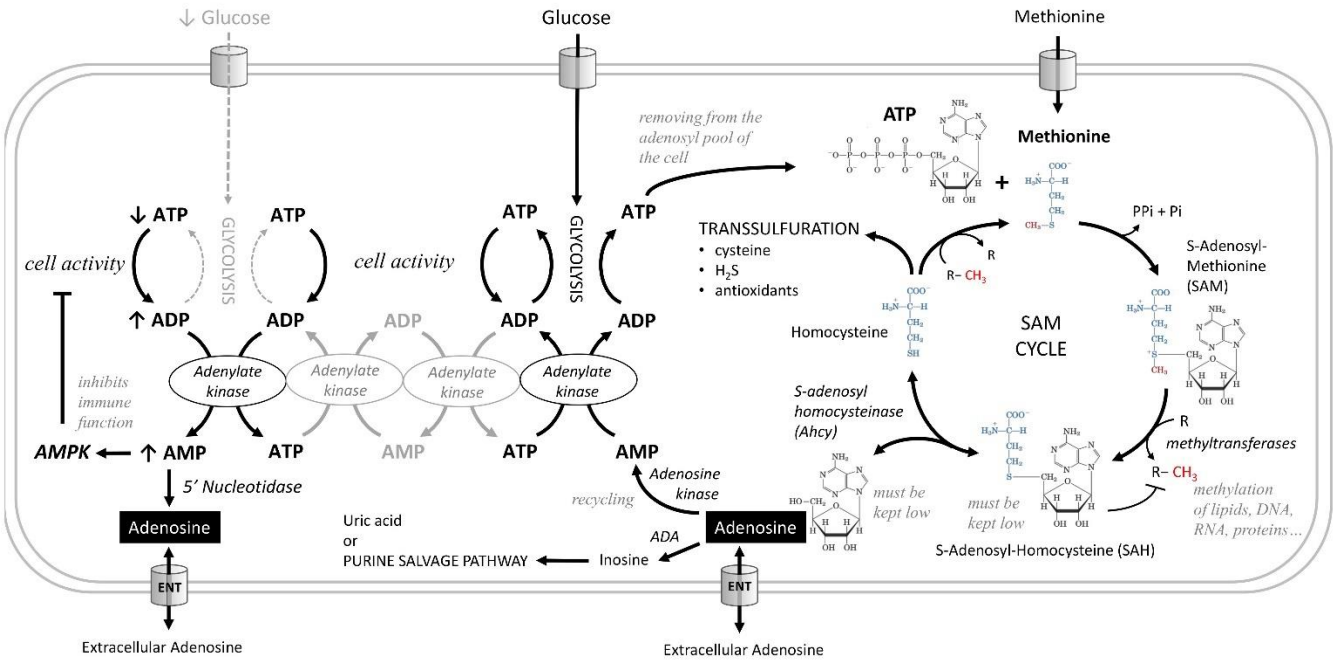

Figure 1. Metabolic pathways producing adenosine.

Adenosine can be produced from AMP by 5'-nucleotidase. AMP increases during metabolic stress, when cells use adenylate kinase to make one ATP and one AMP from two ADP molecules. Increased AMP activates AMP-activated protein kinase (AMPK), which suppresses energy-consuming processes in the cell and activates energy-producing processes, or is converted to adenosine, which can be released from cells via the equilibrative nucleoside transporter (ENT). In the S-adenosylmethionine (SAM) transmethylation pathway, the combination of ATP and methionine produces SAM, the major methyl group donor (red) for the majority of methylations that occur in the cell. During methylation, SAM is converted to S-adenosylhomocysteine (SAH), which is rapidly converted to homocysteine and adenosine by adenosylhomocysteinase (Ahcy), as it would otherwise block further methylation. Ahcy works bidirectionally, and for the "SAM to homocysteine + adenosine" direction to dominate, homocysteine and adenosine must be rapidly metabolized or cleared from the cell. Homocysteine is remethylated back to methionine or further metabolized via the transsulfuration pathway (source of cysteine, H_2S, and antioxidants). The catabolism of adenosine to inosine is mediated by adenosine deaminase (ADA) or recycled to AMP by adenosine kinase which becomes ATP through adenylate kinase, glycolysis or oxidative phosphorylation. Another possible source of adenosine is RNA degradation, which is not shown in this scheme.

127 **RESULTS**

128 **SAM transmethylation pathway accelerates in activated hemocytes**

129 One of the important sources of adenosine in hemocytes is the SAM transmethylation pathway (Figure
130 2A). Putative methionine transporters, as well as all enzymes of this pathway, are strongly expressed in
131 hemocytes, both in the resting and activated state (Figure 2B, Figure 2—figure supplement 1).
132 Methionine can be transported from the hemolymph to the cytosol by *Drosophila* L type amino acid
133 transporters orthologs mnd (CG3297; FBgn0002778), Jhl-21 (CG12317; FBgn0028425), CG1607
134 (FBgn0039844), sbm (CG9413; FBgn0030574), or gb (CG6070; FBgn0039487). The expression of *mnd* and
135 *gb* is particularly high and is further increased during infection (Figure 2B). SAM synthetase (Sam-S;
136 CG2674; EC 2.5.1.6; FBgn0005278) converts methionine and ATP into SAM. SAM is used for methylation
137 by a wide range of methyltransferases (EC 2.1.1.-), or in polyamine synthesis, by SAM decarboxylase
138 (SamDC; CG5029; EC 4.1.1.50; FBgn0019932), producing 5'-methylthioadenosine (MTA). Methylation
139 reactions produce SAH, a potent inhibitor of methyltransferases which must be quickly removed to keep
140 the pathway running. Ahcy (Ahcy; CG11654; EC 3.3.1.1; FBgn0014455) hydrolyzes SAH into adenosine
141 and homocysteine and shows the highest expression among SAM transmethylation pathway enzymes
142 (Figure 2B). AhcyL1 (CG9977; FBgn0035371) and AhcyL2 (CG8956; FBgn0015011), which work as
143 dominant-negative regulators of Ahcy (Parkhitko et al. 2016) have a lower expression and are
144 downregulated during infection (Figure 2B). When adenosine and homocysteine accumulate, Ahcy
145 changes the activity in favor of SAH synthesis. Thus, adenosine and homocysteine must be rapidly
146 metabolized (Kloor and Osswald 2004). Homocysteine can be remethylated back to methionine, by
147 betaine-homocysteine methyltransferase (Bhmt; CG10623; EC 2.1.1.5; FBgn0032727) or homocysteine
148 S-methyltransferase (CG10621; EC 2.1.1.10; FBgn0032726). Alternatively, it is used as a substrate for
149 Cystathionine β-synthase (Cbs; CG1753; EC 4.2.1.22; FBgn0031148) to produce cystathionine (CTH) in
150 the transsulfuration pathway (Figure 2A). Overall, enzymes of the SAM transmethylation pathway, and
151 its associated metabolic branches, are strongly expressed in hemocytes, however, there is no specific
152 pattern of changes upon hemocyte activation during infection (Figure 2B).

153 To analyze SAM transmethylation pathway metabolism, we used high pressure liquid chromatography
154 coupled with tandem mass spectrometry (HPLC-MS/MS). In addition to detecting relative levels of
155 metabolites, 13C-labeled methionine tracing was used to determine methionine usage in the SAM
156 transmethylation pathway in hemocytes of infection and non-infected animals. Hemocytes were
157 extracted by bleeding larvae at 20 hours post infection (hpi). Cells were incubated in media containing
158 0,33 µM $^{13}C_5$ methionine for 20 minutes. This *ex vivo* incubation was designed to resemble physiological
159 conditions. In control larvae, the labeled intracellular methionine fraction reached almost 70% in resting
160 hemocytes and over 80% in activated hemocytes after 20 min of *ex vivo* incubation, demonstrating a
161 substantial uptake of methionine into hemocytes (Figure 2C). Much of this methionine is used for SAM
162 production and methylation, as indicated by the 2-fold increase of SAM and SAH in infected compared
163 to control animals (Figure 2D and E); demonstrating an upregulation of the SAM transmethylation
164 pathway in activated hemocytes. This is further supported by a significantly higher methylation index
165 (ratio of SAM:SAH; Figure 2H-J) in activated hemocytes.

166 SAH is cleaved into homocysteine and adenosine, however, we were unable to reliably detect
167 homocysteine in our metabolomic analysis. Homocysteine can be recycled back to methionine, to enter
168 another round of the SAM transmethylation pathway. In this scenario, fully labeled 13C5 methionine, as

169 was used in this assay, would lead to the formation of methionine m+4. One labeled carbon is used in
170 the methylation reaction while the unlabeled methyl group would be added during recycling (Figure 2A).
171 However, the m+4 portion of the labeled methionine (m+4 and m+5) did not exceed the 3% threshold,
172 set by the methionine labeling impurity (ratio "m+4/[m+4 + m+5]" in the medium was 3%; Figure 2F).
173 This indicates that methionine used for the SAM transmethylation pathway in hemocytes is derived
174 from hemolymph and homocysteine is not remethylated to methionine.

175 To investigate the role of the SAM transmethylation pathway in hemocytes, we knocked down Ahcy by
176 hemocyte-specific RNAi (Figure 2—figure supplement 1 and 2). Ahcy RNAi leads to reduced 13C-labeled
177 methionine uptake in resting hemocytes, although uptake is still increased upon infection (Figure 2C).
178 Methionine incorporation into SAM is significantly lower in activated hemocytes (Figure 2D) and
179 incorporation into SAH is decreased in both, quiescent and activated hemocytes (Figure 2E). These
180 results imply that the SAM transmethylation pathway slows down when there is insufficient Ahcy
181 available. This is reflected in metabolite levels, where SAH is heavily accumulated in Ahcy RNAi
182 hemocytes (Figure 2I) and SAM and methionine levels are higher compared to controls (Figure 2G and
183 H); indicating that they are not metabolized in the SAM transmethylation pathway. This is substantiated
184 by a methylation index that is very low compared to controls, and does not increase upon infection
185 (Figure 2J).

186 SAM can also be utilized for polyamine synthesis that, in addition to polyamines, produces MTA.
187 Polyamines are essential for cell growth and proliferation and participate in various cellular processes
188 (replication, gene expression, biomolecules modifications, etc.). They play a role in macrophage
189 polarization and regulation (Latour, Gobert, and Wilson 2020; Xuan et al. 2023). There is significantly
190 higher incorporation of 13C methionine into MTA in activated hemocytes (Figure 2K) with no changes in
191 MTA level (Figure 2L). Ahcy RNAi hemocytes have increased MTA levels (Figure 2L), which can reflect
192 MTA accumulation, due to decreased SAM transmethylation pathway activity. Decreased 13C
193 methionine incorporation into MTA upon Ahcy knockdown by RNAi (Figure 2K) may be caused by
194 dilution, as unlabeled MTA accumulate (Figure 2L) therefore, we are unable to determine the effect of
195 Ahcy RNAi on polyamine synthesis.

196 The SAM transmethylation pathway is connected to the transsulfuration pathway, which produces
197 cysteine and further antioxidants taurine, and glutathione (Sbodio, Snyder, and Paul 2019). The
198 transsulfuration pathway is one of the ways to metabolically remove homocysteine produced by Ahcy
199 when Cbs converts homocysteine into CTH. This is supported by notable 13C methionine incorporation
200 into CTH (Figure 2M). Interestingly, there is a small, but significant, drop in the labeled CTH fraction in
201 activated hemocytes (Figure 2M), however, this could be due to an overall increase in the level of CTH,
202 including the unlabeled form (Figure 2N). As reported above, the SAM transmethylation pathway is
203 accelerated in activated hemocytes, producing more adenosine, as well as more homocysteine, which
204 must be removed to keep the pathway running. Cystathionine γ-lyase (Cth; CG5345; EC 4.4.1.1;
205 FBgn0000566) usually converts CTH to cysteine. However, this enzyme can also use homocysteine for
206 H_2S production, and was shown to be responsible for homocysteine removal under
207 hyperhomocysteinemia, when Cbs is unresponsive (Singh et al. 2009). H_2S has many diverse roles in the
208 organismal physiology, dependent on its source, localization, and concentration, and has already been
209 connected with immune cells (Sbodio, Snyder, and Paul 2019; Dilek et al. 2020). Based on our
210 transcriptomic data, *Cbs* expression in *Drosophila* larval hemocytes is rather low, and even decreases

211 during infection. Interestingly, *Cth* is strongly expressed, at similar levels to Ahcy. Therefore, our data
212 gives evidence to the clearance of homocysteine by Cth and H_2S production rather than via CTH and Cbs.

213 Knockdown of Ahcy leads to the accumulation of SAH and thus the production of homocysteine, the
214 substrate for CTH, should be strongly inhibited. However, our data shows the relative levels of
215 methionine, as well as the incorporation of 13C methionine into CTH in Ahcy RNAi hemocytes is
216 equivalent to controls (Figure 2M and N). This suggests, there is an alternative connection of methionine
217 with homocysteine and consequently CTH, in addition to Ahcy. Uncovering this alternative connection
218 would be of interest, although it is beyond the scope of this current work.

219 In summary, activated hemocytes increase the uptake of methionine to ramp up the transmethylation
220 pathway. SAM is not only a substrate for methylation, but is also used for polyamine synthesis.
221 Homocysteine is not recycled back to methionine, but is further metabolized in the transsulfuration
222 pathway. Interestingly, our data suggest an alternative link between methionine and CTH independent
223 of Ahcy. Hemocyte-specific Ahcy-RNAi potently suppresses the SAM transmethylation pathway.

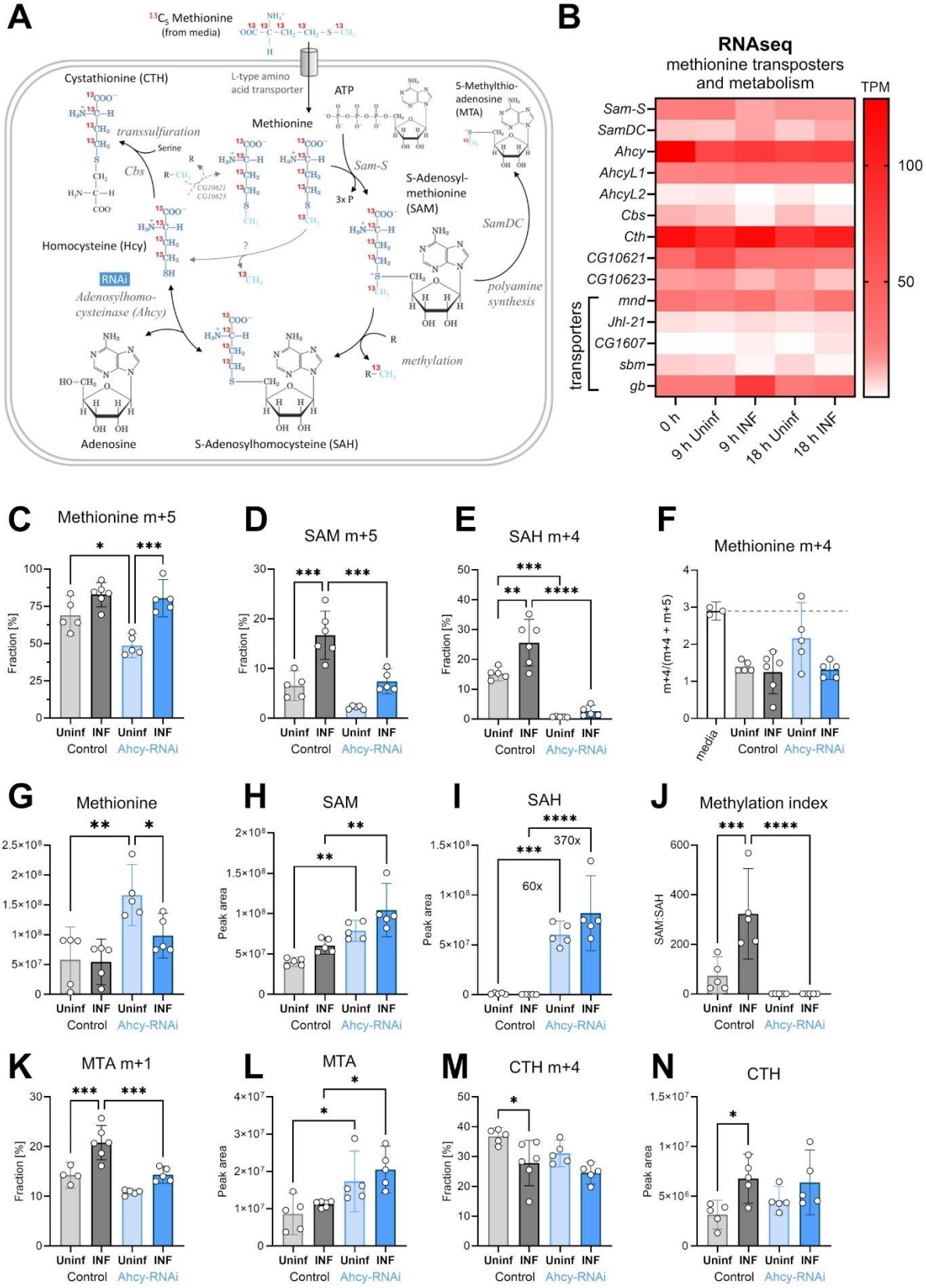
A
13C5 Methionine (from media)
L-type amino acid transporter
Cystathionine (CTH)
transsulfuration
Serine
Cbs
CG10621
CG10623
Methionine
ATP
Sam-S
3x P
S-Adenosyl-methionine (SAM)
5-Methylthio-adenosine (MTA)
SamDC
polyamine synthesis
Homocysteine (Hcy)
RNAi
Adenosylhomo-cysteinase (Ahcy)
methylation
Adenosine
S-Adenosylhomocysteine (SAH)
B
RNAseq
methionine transposters and metabolism
TPM
Sam-S
SamDC
Ahcy
AhcyL1
AhcyL2
Cbs
Cth
CG10621
CG10623
mnd
Jhl-21
CG1607
sbm
gb
transporters
0 h
9 h Uninf
9 h INF
18 h Uninf
18 h INF
C Methionine m+5
D SAM m+5
E SAH m+4
F Methionine m+4
G Methionine
H SAM
I SAH
J Methylation index
K MTA m+1
L MTA
M CTH m+4
N CTH
Fraction [%]
Peak area
m+4/(m+4 + m+5)
SAM:SAH
Uninf INF Uninf INF
Control Ahcy-RNAi
media
60x
370x

224

225 **Figure 2. Analysis of the SAM transmethylation pathway in larval hemocytes by *ex vivo* stable ^{13}C**
226 **isotope tracing**

227 (A) Schematic representation of the SAM transmethylation pathway with polyamine synthesis and
228 transsulfuration branches and labeling with L-methionine-$^{13}C_5$ from media (red 13 represents the
229 labeled carbon). Light blue CH_3 represents the methyl group used during transmethylation or
230 remethylation. Enzymes and processes are italicized. RNAi in blue rectangle represents
231 adenosylhomocysteinase knockdown. (B) Expression heat map (bulk RNAseq) of methionine
232 transporters and enzymes in circulating hemocytes from uninfected (Uninf) and infected (INF) third
233 instar larvae collected at 0, 9 and 18 hpi (0 hpi = 72 hours after egg laying). Means shown in each cell are
234 transcripts per million (TPM) - data in S1_Data. (C-E,K,M) ^{13}C-labeling of metabolites in hemocytes,
235 which were incubated *ex vivo* for 20 min in media containing 0,33 µM L-methionine-$^{13}C_5$. The graphs
236 show the fraction of the compound with one (m+1), four (m+4) or five (m+5) ^{13}C-labeled carbons –
237 methionine m+5 (C), S-adenosylmethionine (SAM) m+5 (D), S-adenosylhomocysteine (SAH) m+4 (E), 5-
238 methylthioadenosine (MTA) m+1 (K) and cystathionine (CTH) m+4 (M). (F) Methionine m+4 portion of
239 total labeled methionine (m+4 and m+5) in media representing the labeling impurity of used methionine
240 (white bar setting threshold - dashed line), and in hemocyte samples. (G-I,L,N) Total levels of methionine
241 (G), SAM (H), SAH (I), MTA (L) and CTH (N) in hemocytes shown as the mean metabolite amounts
242 expressed by the normalized peak area. (J) Methylation index calculated as the ratio of SAM:SAH levels
243 (peak areas in H and I). (C-N) Bars represent mean values with 95% CI of uninfected (Uninf, light grey)
244 and infected (INF, dark grey) control and uninfected (Uninf, light blue) and infected (INF, dark blue)
245 Ahcy-RNAi samples; each dot represents one biological replicate (numerical values in S1_Data and
246 S2_Data); asterisks represent significant differences between samples tested by ordinary one-way
247 ANOVA Tukey's multiple comparison test (*$p<0.05$, **$p<0.01$, ***$p<0.001$, ****$p<0.0001$).
248

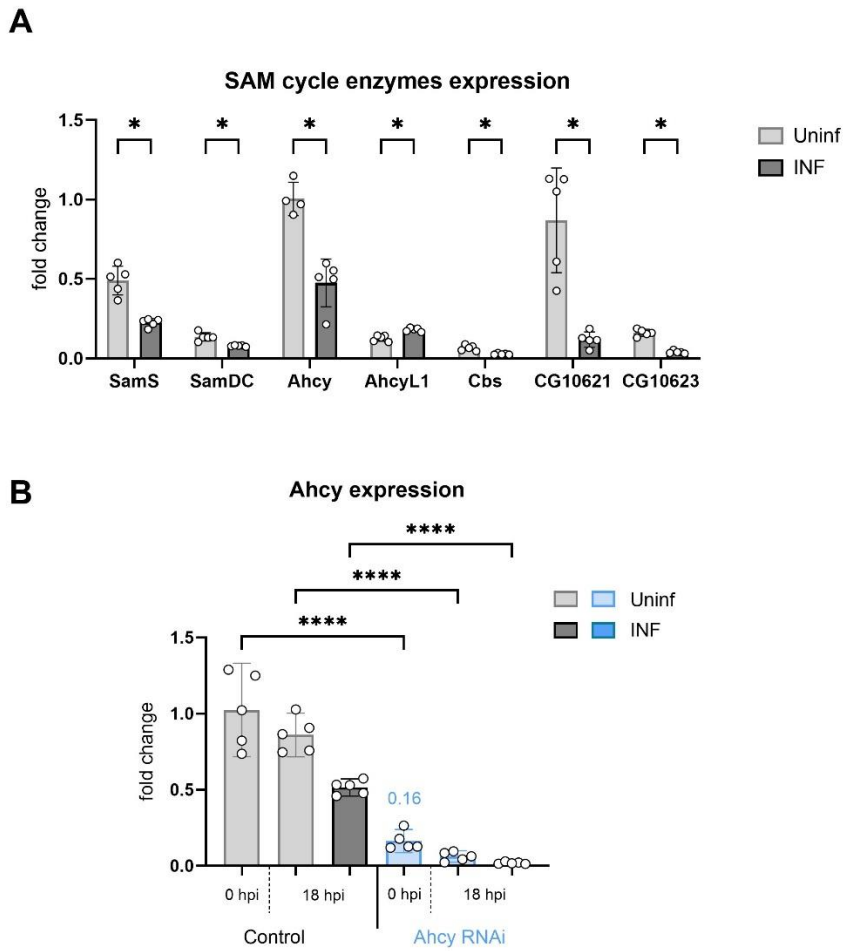

Figure 2-figure supplement 1. Expression of SAM transmethylation pathway enzymes and Ahcy RNAi

(A) Expression analysis of enzymes in the SAM transmethylation pathway in circulating hemocytes from uninfected (Uninf; light gray) and infected (INF; dark gray) third instar larvae collected at 18 hpi by RT-qPCR. Bars show fold change compared to uninfected Ahcy samples (expression levels were normalized to *RpL32* expression in each sample), each dot represents a biological replicate. Asterisks indicate significant differences between samples tested by multiple unpaired t-test. (B) Analysis of Ahcy knockdown efficiency at 0 and 18 hpi by RT-qPCR. RNAi was specifically induced in hemocytes by *SrpD-Gal4 tubP-GAL80ts* driven expression of *UAS-Ahcy-RNAi*^{HMS05799} in larvae maintained at 18°C for the first 3 days of development and then transferred to 25°C. RNAi reduces Ahcy expression to 16% of control at the onset of infection (0 h). Bars represent means with 95% CI of uninfected (Uninf, light gray) and infected (INF, dark gray) control (driver crossed to *P{CaryP}Msp300attP40* control without RNAi) and uninfected (Uninf, light blue) and infected (INF, dark blue) Ahcy-RNAi samples; each dot represents a biological replicate (numerical values in S1_Data); asterisks indicate significant differences between samples tested by ordinary one-way ANOVA Tukey's multiple comparison test (****$p<0.0001$).

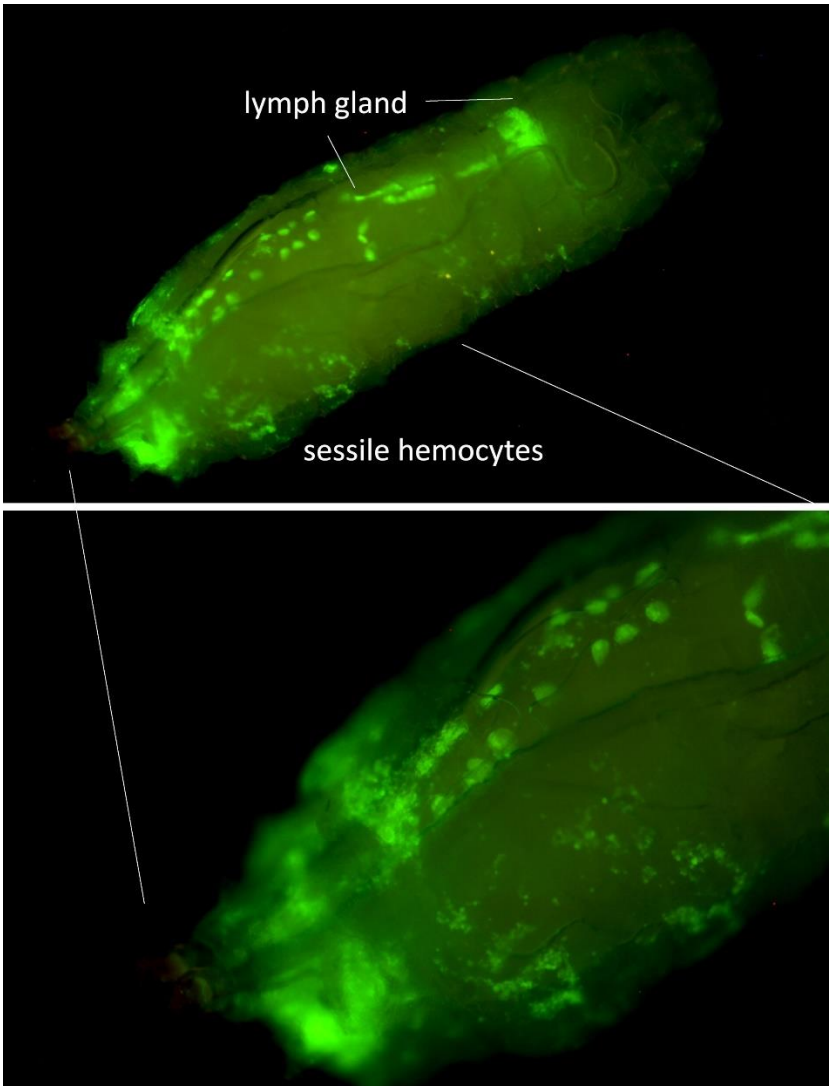

Figure 2-figure supplement 2. Srp-Gal4 Gal80 driver expression

SrpD-Gal4 tubP-GAL80ts driven expression of *UAS-GFP* in 3rd-instar larvae maintained at 18°C for the first 3 days of development and then transferred to 25°C. GFP expression is detected in all lobes of lymph gland, pericardial cells and circulating and sessile hemocytes.

Ahcy produces adenosine as a systemic signal that influences the immune response

In our previous work, we showed that activated hemocytes release increased amount of adenosine (Bajgar et al. 2015; Bajgar and Dolezal 2018). This causes a systemic metabolic switch that slows the organism's development, leaving energy for an effective immune response. Our results show that the SAM transmethylation pathway is enhanced in hemocytes after infection. This means that increased levels of adenosine is produced, as every methylation event results in the production of one adenosine molecule. At the same time, the cell must rapidly remove adenosine, along with homocysteine, to avoid reversing the direction of Ahcy enzyme activity, which would block methylation. This appears to be

279 reflected in the significant reduction in intracellular adenosine levels after infection (Figure 3A). At least
280 part of this reduction is likely due to the release of adenosine from the cell (via the equilibrative
281 nucleoside transporter ENT2 (Bajgar et al. 2015)) since extracellular adenosine levels increase after
282 infection (Figure 3B), as does the level of inosine, which is formed from adenosine by the action of the
283 adenosine deaminase ADGF-A. We measured the extracellular adenosine production in hemocytes after
284 20 minutes of *ex vivo* incubation, when hemocytes were removed by centrifugation and adenosine and
285 inosine were measured in the collected supernatants. We also chose to detect inosine because activated
286 hemocytes produce the adenosine deaminase ADGF-A (Novakova and Dolezal 2011). Therefore, some
287 adenosine is always converted to inosine during sample processing, even when the adenosine
288 deaminase inhibitor EHNA (erythro-9-(2-hydroxy-3-nonly)adenine) is used, otherwise it is difficult to
289 detect any adenosine.

290 Hemocyte-specific Ahcy RNAi leads to a significant decrease in intracellular adenosine levels, confirming
291 that a significant fraction of adenosine is generated by the SAM transmethylation pathway (Figure 3A).
292 However, there is no increase in extracellular adenosine, or inosine levels upon Ahcy knockdown in
293 hemocytes following infection (Figure 3B). This indicates that the SAM transmethylation pathway is
294 responsible for the generation of this extracellular signal. This is further supported by the fact that
295 silencing of Ahcy in hemocytes during infection leads to a significant reduction (by 6 hours) in
296 developmental delay (Figure 3C), the hallmark of systemic effects of adenosine during infection. Similar
297 to our previous work (Bajgar et al. 2015), this results in diminished host defense, which is associated
298 with reduced production of lamellocytes that encapsulate the parasitoid (Figure 3D) and reduced
299 survival (Figure 3E). Interestingly, the induction of Ahcy RNAi in hemocytes accelerates development by
300 approximately 2 hours, even in the absence of infection (Figure 3C), a result similar to silencing ENT2
301 specifically in hemocytes (Bajgar et al. 2015). The normal activity of hemocytes, associated with
302 methylation and adenosine release, appears to slow the overall development of the organism.

303 In summary, the SAM trabsmethylation pathway and Ahcy produce the majority of adenosine in
304 *Drosophila* larval hemocytes and strongly participate in the production of extracellular adenosine as a
305 systemic metabolic regulator. Knockdown of Ahcy in hemocytes reduces larval developmental delay
306 associated with infection, demonstrating the lack in extracellular adenosine production. In addition,
307 knockdown of Ahcy in hemocytes negatively impacts immune response.

308

309

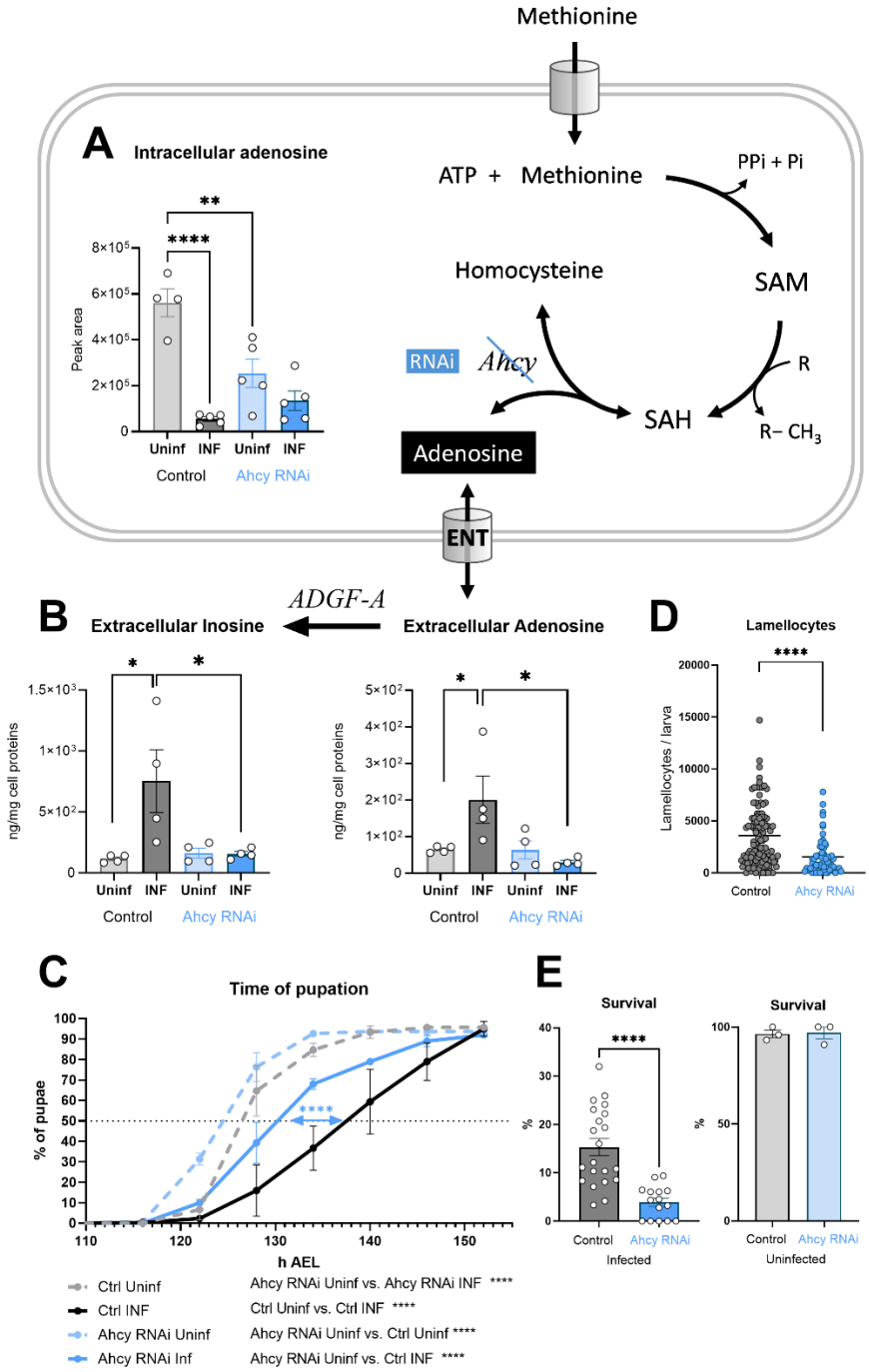

Figure 3. Generation of adenosine in the SAM transmethylation pathway and its systemic effects

(A) Levels of intracellular adenosine in hemocytes shown as the mean metabolite amount expressed by the normalized peak area at 20 hpi. Infection significantly decreases the level in control hemocytes (uninfected - Uninf - light gray vs. infected - INF - dark gray). Hemocyte-specific adenosylhomocysteinase knockdown (Ahcy RNAi; uninfected - Uninf - light blue and infected - INF - dark blue) significantly decreases intracellular adenosine in the uninfected state. (B) Levels of extracellular adenosine (right),

317 released from hemocytes ex vivo after 20 min, and extracellular inosine (left) generated by adenosine
318 deaminase ADGF-A. While infection leads to increased release of adenosine and generated inosine in
319 the control (gray), no such increase is detected with Ahcy RNAi (blue). (C) Pupation is delayed upon
320 infection in control larvae (*n* = 270, uninfected dashed gray line and *n* = 240, infected solid black line) but
321 significantly less in hemocyte-specific Ahcy RNAi larvae (*n* = 260, uninfected dashed blue line and *n* =
322 265, infected solid blue line). Lines represent percentages of pupae at hours after egg laying (h AEL);
323 rates were compared using Log-rank survival analysis. (D) The number of lamellocytes is significantly
324 lower in infected Ahcy-RNAi (blue) larvae compared to infected control (gray). (E) Percentage of infected
325 larvae surviving to adulthood is significantly lower in Ahcy-RNAi (blue) compared to control (gray) while
326 the survival of uninfected individuals is not affected. (A,B,E) Bars represent means with SEM of
327 uninfected (Uninf, light gray) and infected (INF, dark gray) control and uninfected (Uninf, light blue) and
328 infected (INF, dark blue) Ahcy-RNAi samples; each dot represents a biological replicate; (D) dots
329 represent the number of lamellocytes in a larva and the line mean; numerical values are in S1_Data and
330 S2_data; asterisks represent significant differences between samples tested and unpaired t test
331 (*p<0.05, **p<0.01, ***p<0.001, ****p<0.0001).

332

333 **Activated hemocytes recycle ATP and SAM from adenosine**

334 The above results demonstrate that the SAM transmethylation pathway is a major producer of
335 adenosine in activated hemocytes. To maintain methylation, the cell must rapidly remove adenosine,
336 some of which is released from the cell. This, of course, reduces the adenosyl pool of the cell; note that
337 the SAM pathway is a major consumer of ATP when it combines methionine with ATP to form SAM
338 (Figure 4A). Therefore, activated immune cells have active *de novo* purine production, as shown in
339 mammalian macrophages and T lymphocytes (Yu et al. 2019; Roy et al. 2020). Our recent work showed
340 increased pentose phosphate pathway activity is linked with nucleotide production in activated
341 hemocytes (Kazek et al. 2024). However, this is very energy consuming and requires many steps,
342 whereas the recycling of adenosine to AMP requires only one step and one ATP. Ahcy activity has indeed
343 been linked to adenosine kinase activity, which produces AMP from Ado (Moffatt et al. 2002; Xu et al.
344 2017; Murugan et al. 2021). AMP can then be converted to ADP by adenylate kinase (P. Dzeja and Terzic
345 2009) and finally to ATP by glycolysis or OXPHOS, which can again enter the transmethylation pathway.

346 The most striking expression change we detected in activated hemocytes was the increase of adenosine
347 kinase Adk3 (Figure 4B and C) and cytosolic adenylate kinase Ak1 (Figure 4B and D). Another adenosine
348 kinase, Adk2, which is not altered by infection, is also highly expressed in hemocytes, as is the
349 mitochondrial adenylate kinase Ak2 (Figure 4 B-D). Activated hemocytes have a system for recycling
350 adenosine back to ATP, which appears to be further enhanced during infection. The increase of cytosolic
351 Ak1 indicates at least partial redirection of energy metabolism from mitochondria (oxidative
352 phosphorylation) into cytosol (aerobic glycolysis) in activated immune cells (Kornberg 2020).

353 The increase in all levels of IMP, AMP, ADP and ATP (Figure 4E-H) indicates that *de novo* nucleotide
354 production occurs in activated hemocytes. *De novo* purine synthesis may play many different roles in
355 the cell, but an important one is the replenishment of ATP for SAM synthesis. In addition to *de novo*
356 synthesis, our expression analysis suggests that recycling of adenosine to ATP is also involved. We tested
357 this by adding labeled adenosine to resting and activated hemocytes *ex vivo* (Figure 4A). Since
358 hemocytes express ENT2 (Figure 4B and Bajgar et al. 2015), at least some of the labeled adenosine

359 enters the hemocytes and is converted to AMP and finally to ATP (Figure 4I and J). This demonstrates
360 that hemocytes recycle adenosine to ATP, in addition to *de novo* purine synthesis. Both the AMP m+5
361 and ATP m+5 fractions are lower after infection (Figure 4I and J). This is likely due to dilution of the
362 labeled fraction by a significant increase in newly synthesized, unlabeled AMP and ATP (Figure 4F and
363 H). Activated hemocytes also release more adenosine from the cell, so it is possible that it is more
364 difficult for labeled adenosine to enter the cell. Therefore, the extent of ATP recycling from adenosine in
365 resting and activated hemocytes remains elusive.

366 Resting hemocytes show a diminished fraction of labeled SAM derived from labeled adenosine (Figure
367 4K). After infection, there is a significant increase in SAM labeling (Figure 4K), with approximately 13%
368 of labeled ATP molecules being used for SAM synthesis (compare Figure 4J to Figure 4K), while the total
369 level of SAM does not change (Figure 4L). Since ATP is labeled to greater extent in resting hemocytes,
370 this suggests a compartmentalization of the enzymatic cascade physically linking SAM to adenosine
371 recycling (Pedley and Benkovic 2017; Bar-Peled and Kory 2022). If any ATP was used for SAM
372 production, then a higher fraction of labeled ATP in resting hemocytes should be reflected in higher
373 labeled SAM fractions. A higer fraction of labeled SAM in activated hemocytes suggests a physical
374 connection of SAM synthesis and ATP recycling from labeled adenosine. Increased recycling of
375 adenosine to ATP would be characterized by more 13C entering SAM, despite the fraction of labeled ATP
376 appearing lower due to the total amount of ATP produced by *de novo* synthesis.

377 In conclusion, both resting and activated hemocytes recycle adenosine to ATP. Activated hemocytes
378 strongly upregulate the expression of Adk3 and cytosolic Ak1 and increase production of SAM from
379 recycled adenosine.

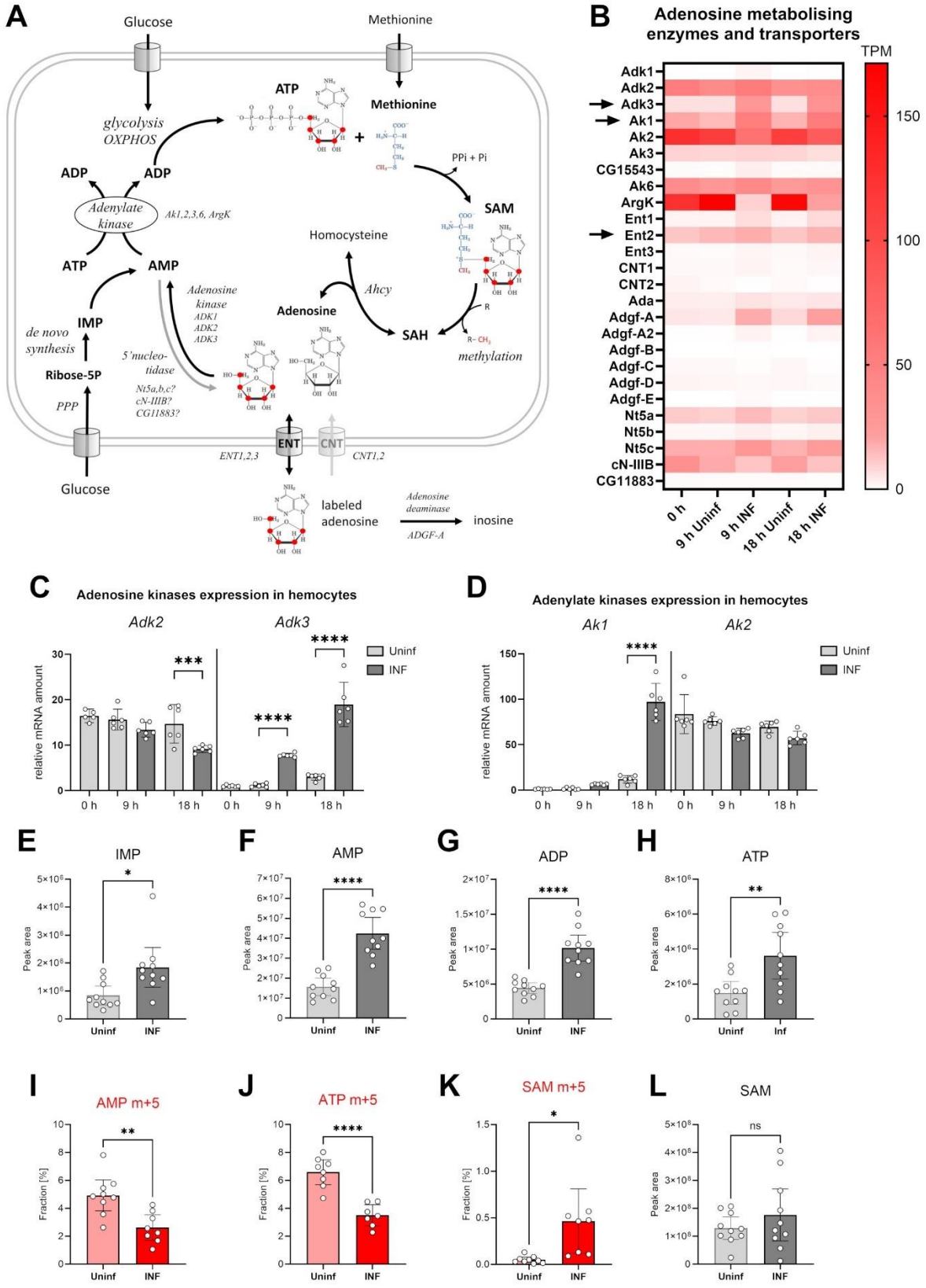
A
Glucose
Methionine
ATP
Methionine
glycolysis
OXPHOS
PPi + Pi
ADP
ADP
SAM
Adenylate kinase
Ak1,2,3,6, ArgK
Homocysteine
ATP
AMP
Adenosine kinase
ADK1
ADK2
ADK3
Ahcy
Adenosine
IMP
de novo synthesis
SAH
methylation
5'nucleo-tidase
Ribose-5P
Nt5a,b,c?
cN-IIIB?
CG11883?
PPP
ENT
CNT
ENT1,2,3
CNT1,2
Glucose
labeled adenosine
Adenosine deaminase
ADGF-A
inosine
B
Adenosine metabolising enzymes and transporters
TPM
Adk1
Adk2
Adk3
Ak1
Ak2
Ak3
CG15543
Ak6
ArgK
Ent1
Ent2
Ent3
CNT1
CNT2
Ada
Adgf-A
Adgf-A2
Adgf-B
Adgf-C
Adgf-D
Adgf-E
Nt5a
Nt5b
Nt5c
cN-IIIB
CG11883
0 h
9 h Uninf
9 h INF
18 h Uninf
18 h INF
C
Adenosine kinases expression in hemocytes
Adk2
Adk3
relative mRNA amount
Uninf
INF
0 h
9 h
18 h
D
Adenylate kinases expression in hemocytes
Ak1
Ak2
E
IMP
F
AMP
G
ADP
H
ATP
Peak area
Uninf
INF
I
AMP m+5
J
ATP m+5
K
SAM m+5
L
SAM
Fraction [%]
ns

380

381 **Figure 4. Analysis of adenosine recycling to SAM in larval hemocytes by *ex vivo* stable ^{13}C isotope**
382 **tracing**

383 (A) Schematic representation of the SAM transmethylation pathway, *de novo* purine synthesis and
384 adenosine recycling to ATP and SAM and labeling with adenosine-$^{13}C_5$ from media (red 13 represents the
385 labeled carbon). Enzymes and processes are italicized. (B) Expression heat map (bulk RNAseq) of
386 adenosine metabolizing enzymes and transporters in circulating hemocytes from uninfected (Uninf) and
387 infected (INF) third instar larvae collected at 0, 9 and 18 hpi (0 hpi = 72 hours after egg laying). Means
388 shown in each cell are transcripts per million (TPM) - data in S1_Data. (C, D) Expression analysis of
389 adenosine kinases Adk2, 3 (C) and adenylate kinases Ak1, 2 (D) in circulating hemocytes from uninfected
390 (Uninf) and infected (INF) third instar larvae collected at 0, 9 and 18 hpi by RT-qPCR. Bars show fold
391 change compared to 0 h Adk3 samples (expression levels were normalized to *RpL32* expression in each
392 sample), each dot represents a biological replicate. (E-H, L) Total levels of IMP (E), AMP (F), ADP (G), ATP
393 (H) and S-adenosylmethionine - SAM (L) in hemocytes shown as the mean metabolite amounts
394 expressed by the normalized peak area. (I-K) ^{13}C-labeling of metabolites in hemocytes, which were
395 incubated *ex vivo* for 20 min in media containing 10 µM adenosine-$^{13}C_5$. The graphs show the fraction of
396 the compound with five ^{13}C-labeled carbons – AMP m+5 (I), ATP m+5 (J) and SAM m+5 (K). (C-L) Bars
397 represent mean values with 95% CI of uninfected (Uninf, light gray or pink) and infected (INF, dark gray
398 or red) samples; each dot represents a biological replicate (numerical values in S1_Data and S2_data);
399 asterisks represent significant differences between samples tested by tested by ordinary one-way
400 ANOVA Sidak's multiple comparison test (C,D) and unpaired t test (E-L) (*p<0.05, **p<0.01, ***p<0.001,
401 ****p<0.0001).
402

403

404 **Adenosine kinase and cytoplasmic adenylate kinase are important for SAM pathway and immune**
405 **response**

406 To determine the importance of adenosine kinase and adenylate kinase, which seem to be necessary for
407 recycling of ATP from adenosine, we again used hemocyte-specific RNAi induced by Srp-Gal4Gal80. Adk3
408 RNAi reduces the infection-induced increase in expression almost 8 times (Figure 5—figure supplement
409 1). Adk3 expression is low in hemocytes of uninfected larvae (Figure 4B and C), thus we did not observe
410 any effect of Adk3 RNAi on the AMP level in uninfected larvae (Figure 5A). However, there is significantly
411 lower level of AMP in hemocytes from the infected larvae (Figure 5A). Adk2 is also strongly expressed
412 both in resting and activated hemocytes (Figure 4C) and that is, most likely, why we still see an infection-
413 induced increase in AMP upon Adk3 RNAi (Figure 5A). This increase is also due to *de novo* purine
414 synthesis. Nevertheless, the increase in AMP in Adk3 RNAi activated hemocytes is significantly smaller
415 than that of controls, indicating that Adk3 activity is important for adenosine conversion to AMP in
416 activated hemocytes. Increase in methylation index is abrogated upon Adk3 RNAi (Figure 5B), showing
417 that Adk3 activity is required for the infection-induced increase in SAM transmethylation pathway. The
418 consequences of Adk3 knockdown phenocopy those of Ahcy knockdown animals, as development is
419 significantly less delayed during infection (Figure 5C) and number of lamellocytes (Figure 5D), as well as
420 survival (Figure 5E) are decreased. We observe similar effects upon cytoplasmic Ak1 knockdown in
421 hemocytes (Figure 5—figure supplement 1), another enzyme upregulated upon infection, which is likely
422 involved in adenosine recycling. The methylation index is abrogated (Figure 5B), development is

423 significantly less delayed during infection (Figure 5F), number of lamellocytes is decreased (Figure 5G)
424 and survival is lower (Figure 5H) upon Ak1 RNAi mediated knockdown. In summary, recycling of
425 adenosine to AMP and potentially to ATP and SAM, using adenosine kinase and cytoplasmic adenylate
426 kinase, appears to be important for activated hemocytes to increase the SAM transmethylation pathway
427 and for effective immune response.

428

429

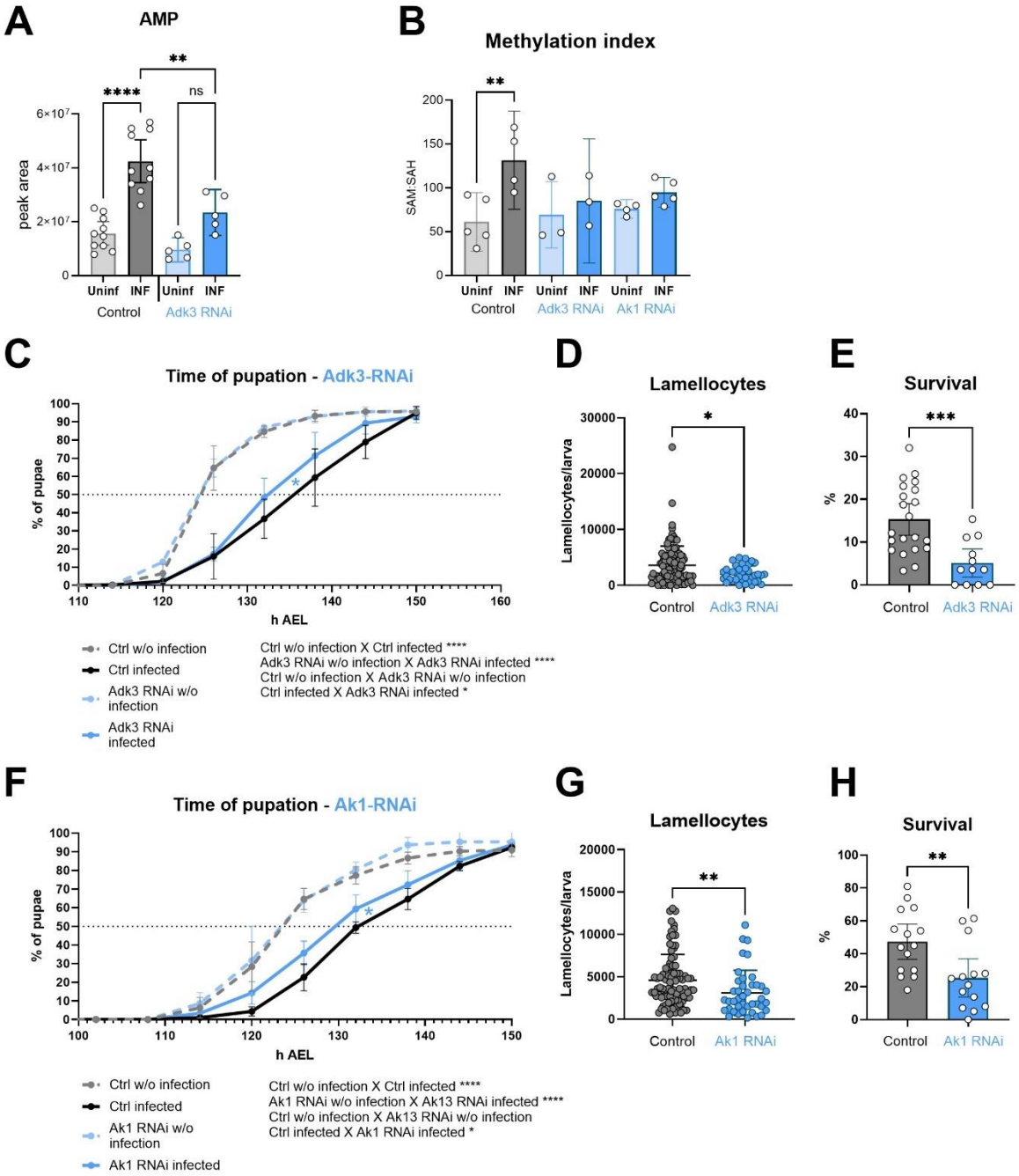

Figure 5. Silencing of adenosine kinase and adenylate kinase in hemocytes affects the SAM transmethylation pathway and immune response

(A) Total levels of AMP in hemocytes shown as the mean metabolite amounts expressed by the normalized peak area. Infection significantly increases the AMP level in control hemocytes (uninfected - Uninf - light gray vs. infected - INF - dark gray). Hemocyte-specific adenosine kinase Adk3 knockdown

437 (Adk3 RNAi; uninfected - Uninf - light blue and infected - INF - dark blue) significantly decreases AMP
438 during infection compared to control. (B) Methylation index, calculated as the ratio of SAM:SAH levels
439 (peak areas; numerical values in S1_Data and S2_data), in control (uninfected - Uninf - light gray and
440 infected - INF - dark gray) and in hemocyte-specific Adk3-RNAi and adenylate kinase Ak1-RNAi
441 (uninfected - Uninf - light blue and infected - INF - dark blue). (C) Pupation is delayed (10 h) upon
442 infection in control larvae (*n* = 270, uninfected dashed gray line and *n* = 240, infected solid black line) but
443 significantly less (7 h) in hemocyte-specific Adk3 RNAi larvae (*n* = 275, uninfected dashed blue line and
444 *n* = 275, infected solid blue line). (D) The number of lamellocytes is significantly lower in infected Adk3-
445 RNAi (blue) larvae compared to infected control (gray). (E) Percentage of infected larvae surviving to
446 adulthood is significantly lower in Adk3-RNAi (blue) compared to control (gray). (F) Pupation is delayed
447 (9 h) upon infection in control larvae (*n* = 225, uninfected dashed gray line and *n* = 270, infected solid
448 black line) but significantly less (6 h) in hemocyte-specific Ak1 RNAi larvae (*n* = 195, uninfected dashed
449 blue line and *n* = 225, infected solid blue line). (G) The number of lamellocytes is significantly lower in
450 infected Ak1-RNAi (blue) larvae compared to infected control (gray). (H) Percentage of infected larvae
451 surviving to adulthood is significantly lower in Ak1-RNAi (blue) compared to control (gray). (A,B,D,E,G,H)
452 Bars/lines represent mean values with 95% CI of uninfected (Uninf, light grey) and infected (INF, dark
453 grey) control and uninfected (Uninf, light blue) and infected (INF, dark blue) Adk3-RNAi or Ak1-RNAi
454 samples; each dot represents one biological replicate (numerical values in S1_Data and S2_data);
455 asterisks represent significant differences between samples tested by unpaired t-test or ordinary one-
456 way ANOVA Tukey's multiple comparison test (*$p<0.05$, **$p<0.01$, ***$p<0.001$, ****$p<0.0001$). (C,F)
457 Lines represent percentages of pupae at hours after egg laying (h AEL); rates were compared using Log-
458 rank survival analysis.

459

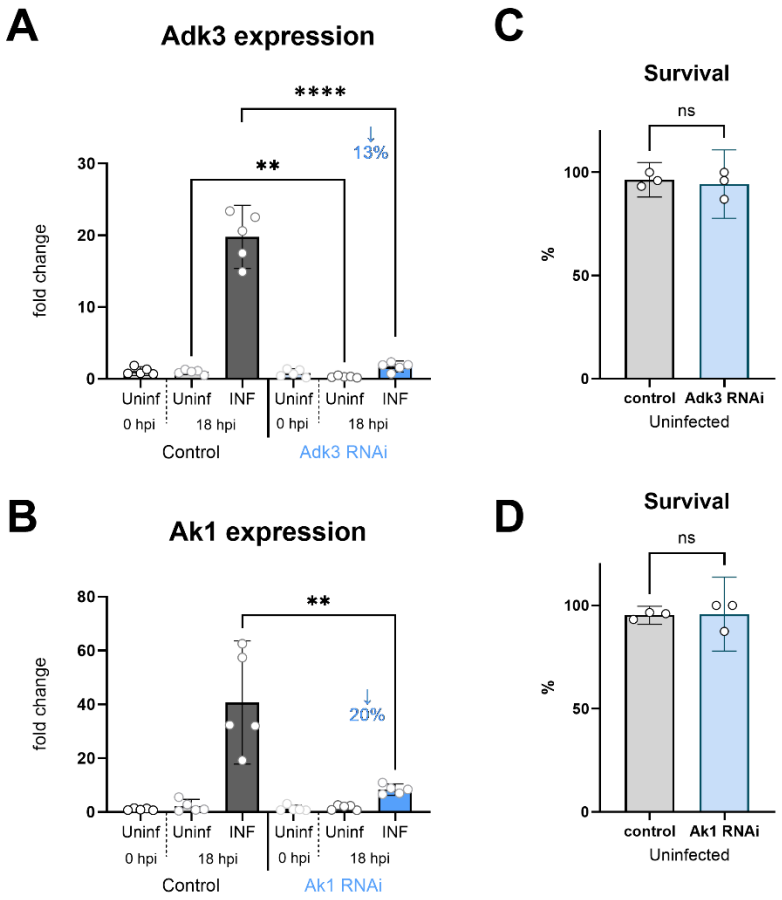

Figure 5-figure supplement 1. Adenosine kinase Adk3 and adenylate kinase Ak1 knockdown efficiency in hemocytes.

Analysis of Adk3 (A) and Ak1 (B) knockdown efficiency at 0 and 18 hpi by RT-qPCR. RNAi was specifically induced in hemocytes by *SrpD-Gal4 tubP-GAL80ts* driven expression of Adk3-RNAi^{HMC06354} or UAS-Ak1-RNAi^{GL00177} in larvae maintained at 18°C for the first 3 days of development and then transferred to 25°C. RNAi reduces Adk3 expression to 13% and Ak1 expression to 20% of control during infection (18 hpi). Bars represent means with 95% CI of uninfected (Uninf, light gray) and infected (INF, dark gray) control (driver crossed to *P{CaryP}Msp300attP40* or *P{CaryP}attP2* control without RNAi) and uninfected (Uninf, light blue) and infected (INF, dark blue) Ahcy-RNAi samples; each dot represents a biological replicate (numerical values in S1_Data); asterisks indicate significant differences between samples tested by ordinary one-way ANOVA Tukey's multiple comparison test (****p<0.0001). Development and survival to adulthood is not affected either by *SrpD-Gal4 tubP-GAL80ts* driven expression of Adk3-RNAi^{HMC06354} (C) or UAS-Ak1-RNAi^{GL00177}(D).

Discussion

We have previously shown that adenosine, released from *Drosophila* hemocytes, is required for systemic metabolic switch and to slow development so that there are enough nutrients for an effective

478 immune response (Bajgar et al. 2015). Here, we show that this signal is generated in hemocytes by the
479 SAM transmethylation pathway, which is enhanced upon infection and is required for the immune
480 response. This novel observation links SAM transmethylation in immune cells to the production of
481 adenosine as a systemic metabolic regulator. In addition, we show that adenosine is not only released
482 from hemocytes but is also recycled to ATP and SAM, mediated by Adk3 and the Ak1, which are
483 necessary for the increase in SAM transmethylation during infection, and therefore effective immune
484 response.

485 The SAM transmethylation pathway is part of the one-carbon metabolism interconnecting the
486 metabolism of serine, glycine, folates, and methionine, supporting *de novo* synthesis of purines and
487 thymidine, and maintaining redox balance. The SAM transmethylation pathway itself controls
488 antioxidant synthesis, sulfur metabolism, polyamine synthesis, and epigenetic programming via
489 methylation (Ducker and Rabinowitz 2017; Vizán, Di Croce, and Aranda 2021). Therefore, Ahcy activity,
490 removing SAH and producing adenosine and homocysteine, is essential, not only for keeping proper
491 function of diverse methyltransferases, but also for a wide range of other essential metabolic processes
492 inside the cell.

493 There is increasing evidence showing the crucial role of the SAM transmethylation pathway in immune
494 cells (Lawson et al. 2012; Klein Geltink and Pearce 2019). It was shown as early as the 80s that peripheral
495 blood mononuclear cells in a "resting" state consume approximately three to five times more SAM for
496 methylation than other, nonhepatic, tissues. Once activated, their SAM consumption is further
497 increased. High SAM utilization was also observed in cultured growing lymphoblasts (German, Bloch,
498 and Kredich 1983). The proper function of the SAM transmethylation pathway and efficient removal of
499 SAH by Ahcy is necessary for chemotaxis in human monocytes, and neutrophils and for lymphocyte
500 effector function (Pike and DeMeester 1988; Zimmerman, Wolberg, and Duncan 1978; Pike, Kredich,
501 and Snyderman 1978). More recently, stable isotope labeling techniques have allowed deeper insight
502 into metabolic set up of activated immune cells. It has been shown that LPS-activated macrophages
503 synergistically increase glycolysis, one carbon metabolism, serine synthesis pathway, pentose phosphate
504 pathway, *de novo* purine synthesis, and SAM transmethylation pathway activity, to induce, and maintain
505 a proinflammatory phenotype. Interestingly, the homocysteine produced by these macrophages is not
506 recycled back into methionine, but SAM synthesis is likely fed exclusively with exogenous methionine
507 transported into the cells (Yu et al. 2019). Roy et al. (2020) demonstrated the metabolic changes that
508 occur in activated CD4+ and CD8+ T lymphocytes. They identified methionine as a crucial metabolite in
509 driving T cells proinflammatory phenotype via epigenetic reprogramming and demonstrated dietary
510 methionine restriction as an effective intervention for autoimmune disease. Activated T lymphocytes,
511 like macrophages, upregulate glycolysis, serine, glycine, and one-carbon metabolism including the SAM
512 transmethylation pathway. These studies indicated that the folate cycle and the SAM transmethylation
513 pathway are uncoupled and homocysteine is not remethylated. Importantly, SAM is synthesized from
514 exogenous methionine and ATP, predominantly produced by *de novo* purine synthesis. Here we show
515 that in *Drosophila* immune cells, SAM is also synthesized mostly from exogenous methionine, and
516 homocysteine is not remethylated back to methionine, but rather used in transsulfuration pathway.
517 Interestingly, our results also suggest an alternative means of CTH production from methionine,
518 independent of Ahcy, although this is not further explored here. Activated hemocytes also increase *de*
519 *novo* purine synthesis, supported by increased pentose phosphate pathway activity (Kazek et al. 2024).

520 Ahcy was shown to play an important role in adenosine production in heart muscle cells, under
521 normoxic conditions (Lloyd et al. 1988; Deussen 1989). Adenosine produced by Ahcy contributes to
522 viability of hepatocellular carcinoma cells (HepG2), since Ahcy knockdown followed by adenosine
523 depletion leads to activation of the DNA damage response, cell cycle arrest, a decreased proliferation
524 rate and DNA damage (Belužić et al. 2018). However, the adenosine formed in the SAM
525 transmethylation pathway is usually referred to in studies as a by-product that needs to be removed
526 quickly to avoid Ahcy reverse function, which would block further methylation. Here, we show that
527 adenosine formed in the SAM transmethylation pathway is not a mere by-product but can have a
528 significant impact on the immune response and the physiology of the whole organism. With the increase
529 of SAM transmethylation pathway activity in activated hemocytes, more adenosine is produced. As
530 intracellularly adenosine decreases, it is released to the extracellular space; this leads to suppression of
531 metabolism in non-immune tissues, and consequently a development delay. This metabolic suppression
532 is crucial for redirecting nutrients towards the immune system and mounting an effective immune
533 response. Knockdown of Ahcy by RNAi suppresses the infection-induced increase in extracellular
534 adenosine, as well as the delay in development, demonstrating that this important systemic signal is
535 indeed generated by the SAM transmethylation pathway. It is important to add that while adenosine-
536 mediated metabolic suppression and developmental delay are important for an effective immune
537 response, it is more likely that the ineffective immune response in Ahcy RNAi animals is due to
538 suppression of the SAM transmethylation pathway itself in hemocytes, which is required for their
539 function. At the same time, we do not want to suggest that SAM transmethylation in hemocytes is the
540 only source of adenosine during infection. Ectoenzymes are an important source of extracellular
541 adenosine that convert extracellular ATP to ADP, AMP and adenosine. This cascade is an important
542 immunomodulator in mammals (Antonioli, Pacher, and Haskó 2022). *Drosophila* also has this cascade of
543 ectoenzymes (Fenckova et al. 2011), which appears not to have an immunomodulatory role, likely due
544 to more rudimentary adenosine signaling (Dolezelova et al., 2007), but could still serve as a source of
545 extracellular adenosine. Nevertheless, the absence of extracellular adenosine increase and reduced
546 developmental delay upon hemocyte-specific knockdown of Ahcy clearly demonstrates the essential
547 role of the SAM transmethylation pathway in generating of adenosine as a systemic signal.

548 After ATP, SAM is the most used substrate in the cell, with up to half of the daily methionine intake in
549 humans used for SAM synthesis, the vast majority of which is used for methylation (Lu 2000). If all the
550 adenosine produced by Ahcy was released to hemolymph, hemocytes would likely lose a huge amount
551 of ATP due to SAM synthetase utilizing the adenosyl group of ATP and methionine to create SAM.
552 Increased ATP consumption by the accelerating the SAM transmethylation pathway must be supported
553 by *de novo* purine synthesis. Previous work (Kazek et al. 2024) as well as results presented here, show
554 increased *de novo* purine synthesis in activated immune cells. However, this consumes a considerable
555 amount of energy (6 ATP for one IMP molecule) and takes eleven steps to produce IMP from the initial
556 ribose-5-phosphate. Thus, it is more efficient to recycle at least some ATP from the adenosine generated
557 in the SAM transmethylation pathway via coordinated action of adenosine kinase, cytosolic adenylate
558 kinase, and glycolysis. This is in line with ATP synthesis from adenosine via AMP and ADP shown to be
559 significantly increased in activated rat peritoneal macrophages (Barankiewicz and Cohen 1985).

560 Adenosine kinase has been shown to be coupled with Ahcy to effectively remove adenosine and keep
561 the SAM transmethylation pathway running (Moffatt et al. 2002; Xu et al. 2017; Murugan et al. 2021).
562 Subsequently, the AMP produced can be utilized by the adenylate kinase catalyzing phosphoryl

563 exchange reaction AMP + ATP ↔ 2 ADP. Adenylate kinase is crucial for cellular energy homeostasis, by
564 regulating nucleotides ratio, AMP production and direction to diverse metabolic sensors (e.g. AMPK). In
565 addition, it is responsible for the transfer of ATP energy rich phosphoryl between energy producing and
566 energy utilizing sites by a sequence of repeated reactions, creating an effective energy transfer shuttle
567 across the cell (R. J. Zeleznikar et al. 1990; Robert J. Zeleznikar, Dzeja, and Goldberg 1995; P. P. Dzeja,
568 Chung, and Terzic 2007; P. Dzeja and Terzic 2009). Our hemocyte RNAseq and qPCR data show that
569 *Drosophila* Adk3 and Ak1 are expressed at low levels in quiescent hemocytes, but their expression
570 increases dramatically during infection. Experiments using 13C labeled adenosine show its incorporation
571 into AMP, ADP, ATP, and especially into SAM, in which the incorporation is significantly increased upon
572 hemocyte activation. These results connect adenosine recycling with the SAM transmethylation
573 pathway. Without infection, the methylation index of Adk3 and Ak1 RNAi in hemocytes is the same as in
574 control cells. However, upon infection, there is no increase in the methylation index in Adk3 and Ak1
575 RNAi cells. When the SAM transmethylation pathway is not accelerated, Ahcy does not produce more
576 adenosine, and consequently the adenosine-induced developmental delay during infection is reduced in
577 Adk3 and Ak1 RNAi, whereas without infection, RNAi larvae develop at the same rate as controls. Our
578 results therefore demonstrate a novel functional connection of adenosine recycling to ATP with SAM
579 transmethylation pathway. At least under energy demanding conditions, as during the activation of
580 immune cells, Adk and cytosolic Ak activities appear to support SAM transmethylation pathway activity.

581 Similar to Ahcy RNAi, Adk3 and Ak1 RNAi in hemocytes also negatively affects immune response
582 efficiency. We see a significant decrease in lamellocytes number in our infected knockdown larvae,
583 resulting in decreased survival. It is important to note, that while Ak1 RNAi most likely also affects *de*
584 *novo* purine synthesis, the Adk3 RNAi effects we observed are due to impairments in adenosine
585 recycling. Connecting the SAM transmethylation pathway-driven production of adenosine with its
586 recycling via Adk3 and Ak1 leads us to following hypothesis (Figure 6):

587 Most cellular processes involve methylation, therefore the SAM transmethylation pathway reflects the
588 activity of the cell. While a wide variety of molecules are methylated, adenosine is the universal product
589 of each individual methylation. Thus, adenosine production reflects the sum of all methylations (where
590 SAM has been used) and therefore the overall activity of the cell. Adenosine must be removed quickly as
591 to not block the SAM transmethylation pathway. The preferred fate is to recycle adenosine to AMP and
592 eventually ATP so that the cell does not lose its adenosyl pool. However, this requires nutrients,
593 adenosine kinase requires ATP, adenylate kinase produces ADP from AMP and ATP and the resulting
594 ADP is recycled to ATP in glycolysis, consuming glucose. If the cell's nutrient supply is inadequate, AMP
595 begins to accumulate, due to the opposite action of adenylate kinase, preventing adenosine from being
596 recycled to AMP by adenosine kinase. In this case, the accumulating adenosine is pushed out of the cell
597 via ENT, where it becomes a signaling molecule, informing surrounding tissues of the need for more
598 nutrients. We therefore look at adenosine as a sensitive sensor of the balance between cell activity
599 (reflected in methylation) and nutrient supply - the better the balance, the less adenosine is released
600 and the more is recycled.

601 To experimentally test this hypothesis will require extremely well controlled conditions, as offered for
602 example by uniform cell culture in precisely controlled media, and delicate manipulation of the
603 important players. The proposed role of adenosine as a sensitive sensor between cell activity and
604 nutrient supply might have far-reaching implications. The production of adenosine by nucleotidase as
605 the ADP/ATP ratio rises is known, for example, to generate a signal in ischemic tissue to inform

surrounding tissues of metabolic stress (e.g., vasodilation to increase blood flow). However, the generation of such a signal as a result of an imbalance between cell activity and nutrient supply is a novel and exciting hypothesis.

The fate of adenosine is determined by biochemical properties and the expression of enzymes and transporters. The Km values of *Drosophila* Adk2 and Adk3 are not known (Fleischmannova et al. 2012; Stenesen et al. 2013), but it is possible that they differ, and that increased expression of Adk3 specifically during infection is important in readjusting the balances between AMP and adenosine, which are determined by the properties of nucleotidases and adenosine kinases (Boison 2013). The expression levels and properties of nucleoside transporters and adenosine deaminase also play important roles. The specific setup of this whole system in certain cell types under certain conditions determines what happens with adenosine (Dulla and Masino 2013; Dale 2021). Studying this setup is essential to understanding the role of this system in specific situations, such as those in which adenosine may be generated by imbalances in activity and energy supply. For example, does it play a role in the early activation of immune cells, regulating nutrient supply to their site of activation? In addition, in the tumor microenvironment, adenosine inhibits infiltrating immune cells (Boison and Yegutkin 2019). Until now adenosine ectoenzymes have been mainly studied in this respect. However, the SAM transmethylation pathway is very active in tumor cells (Vizán, Di Croce, and Aranda 2021) - can tumors regulate their environment by releasing adenosine, which is produced according to our hypothetical mechanism?

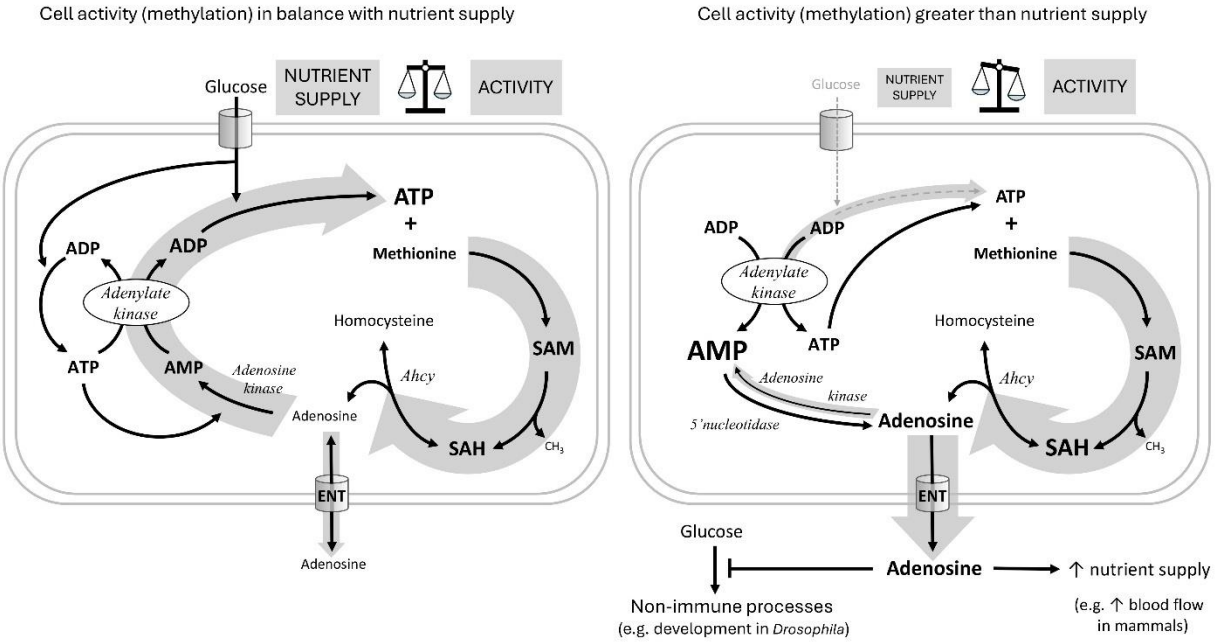

Figure 6. Hypothetical role of adenosine as a sensor of the balance between cell activity and nutrient supply

629 The hypothetical scheme shows an immune cell with either sufficient (left) or insufficient (right) nutrient
630 supply for the given cellular activity. For each individual transmethylation event using S-
631 adenosylmethionine (SAM) as a methyl group donor and producing S-adenosylhomocysteine (SAH), S-
632 adenosylhomocysteinase (Ahcy) generates one molecule of adenosine (and homocysteine). Adenosine
633 thus reflects the sum of all SAM transmethylations in the cell and may be considered as a proxy for cell
634 activity (thick gray arrow on the right). If there are enough nutrients (cell on the left) to maintain high
635 levels of ATP, adenosine can be recycled first to AMP by adenosine kinase, which requires the first ATP,
636 then to ADP by adenylate kinase, which requires the second ATP, and finally to ATP by glycolysis (or
637 oxidative phosphorylation) using glucose (the gray arrow on the left as thick as the one on the right
638 expresses the balance). Recycled ATP can then enter the next round of transmethylation with
639 methionine to form SAM. If there are not enough nutrients (cell on the right, thin gray arrow on the left)
640 to regenerate ATP from ADP, ATP is produced from two ADP molecules by adenylate kinase,
641 simultaneously generating AMP. Accumulated AMP prevents adenosine recycling by adenosine kinase
642 (thin gray arrow on the left), and on the contrary, more adenosine can be produced from AMP by
643 5'nucleotidase. In this case, adenosine is pushed out of the cell (thick gray arrow down) via the
644 equilibrative nucleoside transporter (ENT) and becomes an extracellular signaling molecule. Extracellular
645 adenosine can, for example, suppress the development of Drosophila larvae or increase blood flow in
646 mammals to provide more nutrients to immune cells.

647

648 **Methods**

649 **Fly strains, cultivation, and parazitoid wasp infection**

650 *Drosophila melanogaster* strain w^{1118} (FBal0018186) in Canton S genetic background (FBst0064349) was
651 used as a control line unless otherwise stated. Strains *UAS-Ahcy-RNAi* $Ahcy^{HMS05799}$ (FBti0186788), UAS-
652 Adk3-RNAi $Adk3^{HMC06354}$ (FBti0185498), UAS-Adk2-RNAi $Adk2^{GL00036}$ (FBti0144142), UAS-Ak1-RNAi
653 $Ak1^{GL00177}$ (FBti0144266), and control lines for RNAi y^1 v^1; *P{CaryP}attP2* (FBst0036303), and y^1 v^1;
654 *P{CaryP}Msp300attP40* (FBst0036304) were obtained from the Bloomington Drosophila Stock Center.
655 The *SrpD-Gal4* strain (FBtp0020112) was obtained from M. Crozatier, backcrossed into the w^{1118}
656 background, and recombined with P{tubP-GAL80ts}2 (FBti0027797), which was also backcrossed into
657 w^{1118} background, to generate the w^{1118}; +/+; *SrpD-Gal4* P{tubP-GAL80ts}2 line with Gal4 expression in
658 all hemocytes but not in the fat body when kept at 18°C for the first 3 days of development and then
659 transferred to 25°C (S Fig; expression in the fat body is only present at 29°C in this line). All flies were
660 grown on cornmeal medium (8% cornmeal, 5% glucose, 4% yeast, 1% agar, 0.16% methylparaben) at
661 25°C. Parasitoid wasps *Leptopilina boulardi* were reared on sugar agar medium (6% sucrose, 1.5% agar,
662 0.75% methylparaben) and grown by infection of wild-type *Drosophila* larvae. Early third instar larvae
663 (72 hours after egg laying) were infected with parasitoid wasps (= time point 0 hours). Weak infection
664 (1-2 eggs per larva) was used for survival analysis. Strong infection (4-8 eggs per larva) was used for the
665 rest of the experiments to obtain a strong and more uniform immune response. Infections were
666 performed on 60-mm Petri dishes with standard cornmeal medium for 15 minutes for weak infection
667 and 45 minutes for strong infection.

668

669 **Hemocyte counting**

670 *Drosophila* hemocytes were counted at 20 hpi by bleeding one larva in 15 µL of PBS and using Neubauer
671 hemocytometer (*Brand GMBH*) using differential interference contrast microscopy. Particular types of
672 hemocytes were determined based on the cell morphology.

673

674 **Survival and developmental time analysis**

675 Infected and non-infected 3rd instar larvae were placed into fresh vials in a number of 30 larvae per vial,
676 3 vials per genotype with 3 to 5 independent experiments. Differences in larval development were
677 determined by counting newly appeared pupae every 6 hours post infection. Percentage of pupae
678 number per total used larvae number at particular time points was plotted and compared by Log-rank
679 test. For survival, all emerged adult flies were counted and checked if they contain the melanized eggs
680 to confirm they were infected. The ones without any egg were excluded from the analysis. Percentage of
681 emerged adults number per total used infected individuals were plotted.

682

683 **Gene expression analysis**

684 Based on the larval stage, 30 to 50 larvae were washed 3x in PBS, transferred on microscope slide
685 covered with parafilm and placed on ice. All larvae were opened with tweezers and released
686 hemolymph with hemocytes were aspired with 10 µL pipette and transferred into 1.5 mL tube
687 containing TRIzol Reagent (*Life Technologies*) for RNA extraction. RNA was purified with Direct-zol RNA
688 Microprep (*Zymo-Research*). Total RNA was used for cDNA preparation by PrimeScript Revrese
689 Transcriptase (*Takara*) with oligo(dT) primer. cDNA was used as a template for qPCR using TP SYBR 2x
690 Master Mix (*Top-Bio*) and C1000 Touch Thermal Cycler (*Bio-Rad*). Expression of a specific gene in each
691 sample was normalized to expression of *RpL32* (FBgn0002626) and relative gene expression was
692 counted with ΔΔCt method. Graphs showing target gene expression and statistical analysis were made
693 with GraphPad Prism.

694

695 Primers:

Ahcy	Fw	AAGCTGTCGCACAAATGGCG
	Rev	GCACGTTGTGCACCAGGAAC
AhcyL1	Fw	GGCGAGACGGAAGAGGACT
	Rev	AGAGAGCTGATAGAGACGGTG
Adk2	Fw	AACTTCACCATCGATCACCTGG
	Rev	TAGGAACGGTCGCTGTTTGG
Adk3	Fw	CTGGACATGGAGAAACTCAACC
	Rev	AAAGAAGAGCGCGTCTGTGC

Ak1	Fw	CTCGGCATTGATCGTAAGGG
	Rev	CGATCTGGCGCTGTACTTTG
Ak2	Fw	GCTGAGAAGCTCGACACATTG
	Rev	CTCCAGTGACATCGTCCGTC
Ak3	Fw	GATCCAGCGATTCTTGACCC
	Rev	CGGATAACCGAGGTAGGCAAC
ArgK	Fw	ATGGAGATGATGCGGAGATG
	Rev	TCGACGACCACTTCCTGTTC
Cbs	Fw	AGATTACGCCCAACATCCTCG
	Rev	AATGCGGTCCTTCACTGATCC
CG10621	Fw	CATCGAGCTGATAAAGAACACGG
	Rev	AATGGAGGCAATGATCAAAGGG
CG20623	Fw	ATGCCAAATTCTGGGTCTCCC
	Rev	AAAGGGGTCACGAATAGTGGG
RpL32	Fw	AAGCTGTCGCACAAATGGCG
	Rev	GCACGTTGTGCACCAGGAAC
SamDC	Fw	CAACGGTGACGATGATCTGC
	Rev	AGTTTTAAGGATCCATCGTCGC
SamS	Fw	CAAATCAGCGACGCTATCTTGG
	Rev	TGTCTCACGAACAACCTTCTGG

Bulk RNAseq analysis

RNA was extracted from circulating hemocytes (72 hours after egg laying = time of infection = 0 hours, 81 hours after egg laying = 9 hours post infection/hpi and 90 hours after egg laying = 18 hpi) of uninfected and infected 3rd instar *w*^{1118} larvae and processed as described in details with all data in (Kazek et al. 2024). Raw data are available at The European Nucleotide Archive under study accession number: PRJEB74490 (secondary acc: ERP159178) (https://www.ebi.ac.uk/ena/browser/view/PRJEB74490).

Metabolomics and stable 13C isotope tracing in hemocytes ex vivo

706 Samples for metabolomics were collected 20 hours post infection. Larvae were washed first with
707 distilled water and then with PBS to reduce contamination. Larval hemolymph was collected by carefully
708 tearing the larvae on a glass microscope slide covered with parafilm. Hemolymph from 100 larvae was
709 immediately collected into sterile 1.5 ml Eppendorf polypropylene centrifuge tubes prefilled with 100 µl
710 PBS and centrifuged for 5 min at 25°C, 360xg. For experiments without 13C isotope tracing, hemocytes
711 were resuspended in 50 µL of HPLC water and three times frozen in liquid nitrogen/thawed at 37 °C
712 (established for sufficient cell disruption and extraction of intracellular metabolites). 200 µl of cold
713 acetonitrile-methanol (1:1) was added and stored at -80 °C until LC-HRMS analysis described in Kazek et
714 al. 2024. For experiments with 13C isotope tracing, the supernatant was removed and the cells were
715 mixed with medium containing PBS, 5 mM trehalose, 0.5 mM glucose, 5 mM proline, 5 mM glutamine
716 (*Sigma/MERCK*), supplemented with gentamicin (10 mg/ml; *Gibco*), amphotericin B (250 µg/ml; *Gibco*)
717 and 0.1 mM phenylthiourea (PTU; *Sigma/MERCK*) to prevent melanization. Based on the experiment,
718 medium further contained either 0,33 µM L-methionine-$^{13}C_5$ or 10 µM adenosine-$^{13}C_5$ and unlabeled
719 0,33 µM L-methionine. The hemocytes were then incubated *ex vivo* for 20 min at 25°C and 80-90%
720 humidity. The cells were then centrifuged for 5 min at 25°C, 360xg, the supernatant was removed, the
721 cells were mixed with 50 µl of cold PBS and frozen in liquid nitrogen/thawed at 37°C three times (to
722 disrupt the rigid hemocyte cells). Finally, 200 µl of cold acetonitrile-methanol (1:1) was added, in
723 addition, the internal standard 4-fluorophenylalanine (50 ng/sample) was added to control the
724 extraction efficiency and mass spectrometer responses and samples were stored at -80°C until LC-HRMS
725 analysis which is described in Kazek et al. 2024. When extracellular adenosine and inosine were
726 measured, samples were collected in room temperature and centrifuged in 25°C, 5 min, 360xg to wash
727 hemocytes from hemolymph and extracellular metabolites. Cells were resuspended in medium
728 composed of PBS, 5 mM trehalose, 0.5 mM glucose, 5 mM proline, 5 mM glutamine, 0.33 mM
729 methionine (*Sigma/MERCK*), supplemented with gentamicin (10 mg/ml; *Gibco*), amphotericin B (250
730 µg/ml; *Gibco*), 0.15 mM EHNA (*Sigma/MERCK*) and 0.1 mM phenylthiourea (PTU; *Sigma/MERCK*) to
731 prevent melanization. Samples were incubated for 20 minutes in room temperature, and then
732 centrifuged in 4°C, 5 min, 360xg. 70 µL of supernatant were transferred into new sterile 1.5 mL
733 Eppendorf polypropylene centrifuge tube containing 70 µL of acetonitrile and stored at -80 °C until LC-
734 HRMS analysis. Pelleted cells were stored in -80°C for protein measurement with QuantiPro™ BCA Assay
735 Kit (*Sigma/MERCK*).

736 Raw data are available at https://doi.org/10.6084/m9.figshare.27291300.v1 and processed data in
737 S2_Data. For peak area analysis, the data were normalized to the total content of all screened unlabeled
738 metabolites - the peak area of the metabolite in a particular sample was divided by the peak area of the
739 same metabolite of the selected reference sample and this procedure was repeated for each individual
740 unlabeled metabolite. These ratios of all metabolites in one particular sample were averaged to
741 determine a normalization factor. We then divided the measured peak area by the normalization factor
742 for that sample to obtain the normalized peak area values (normalization factors are reported in
743 S2_Data).

744

745 **Data analysis**

746 Data were analyzed and graphed using GraphPad Prism (*GraphPad Software*), with specific statistical
747 tests shown in the legend of each figure.

Acknowledgments

The authors acknowledge funding from the Grant Agency of the Czech Republic to TD (Projects 17-16406S and 20-09103S; www.gacr.cz) and from the Grant Agency of the University of South Bohemia in České Budějovice to PN (087/2019/P). We thank Dr. Michele Crozatier and Bloomington Drosophila Stock Center for fly and wasp stocks. We thank Dr. Michalina Kazek for help with metabolomics optimization, to Lucie Hrádková for laboratory management and Marcela Jungwirthová for project management, and all members of Doležal and Moos laboratories for their help with work. We thank Dr. Adam Bajgar for help with bulk RNAseq and Dr. Vladimír Beneš and Genomics Core Facility (EMBL Heidelberg, Germany) for RNAseq services and Dr. Bajgar and Dr. Gabriela Krejčová for help with optimization of the molecular biology methods and wasp infections and general manipulation with flies and larvae. We thank Dr. Ellen McMullen for manuscript editing.

Additional files

S1 Data. Raw data/numerical values for data presented in graphs.

The MS Excel file containing the data used to generate the plots in Figure 2, 3, 4, 5 and Figure 2-figure supplement 1 and Figure 5-figure supplement 1. The data for each figure are shown on individual sheets of this file with the panel number indicated next to the data.

S2 Data. Metabolomics and stable ^{13}C isotope tracing in circulating hemocytes during parasitoid wasp infection.

MS Excel sheets with stable ^{13}C isotope tracing experiments. List of metabolites, their characterizations, identification, HPLC/HRMS parameters is on the first sheet [List of Metabolites]. Data from the following experiments are in individual sheets (values are raw or normalized areas under respective chromatographic peaks): [S1] Peak area of metabolites of interest for control and Ahcy RNAi hemocytes. [S2] – Combination of quantitative analysis (ng/sample) and peak area of metabolites of interest for control and Ahcy RNAi hemocytes incubated with 13C5 methionine. [S3] Peak area of metabolites of interest for control and Adk3 RNAi and Ak1 RNAi. [S4] Combination of quantitative analysis (ng/sample) and peak area of metabolites of interest for control and Adk3 RNAi and Ak1 RNAi hemocytes incubated with 13C5 adenosine. Raw data are available at figshare (https://doi.org/10.6084/m9.figshare.27291300.v1).

REFERENCES

Antonioli, Luca, Pál Pacher, and György Haskó. 2022. "Adenosine and Inflammation: It's Time to (Re)Solve the Problem." *Trends in Pharmacological Sciences* 43 (1): 43–55. https://doi.org/10.1016/j.tips.2021.10.010.

Bajgar, Adam, and Tomas Dolezal. 2018. "Extracellular Adenosine Modulates Host-Pathogen Interactions through Regulation of Systemic Metabolism during Immune Response in Drosophila." Edited by Brian P. Lazzaro. *PLOS Pathogens* 14 (4): e1007022. https://doi.org/10.1371/journal.ppat.1007022.

Bajgar, Adam, Katerina Kucerova, Lucie Jonatova, Ales Tomcala, Ivana Schneedorferova, Jan Okrouhlik, and Tomas Dolezal. 2015. "Extracellular Adenosine Mediates a Systemic Metabolic Switch during Immune Response." Edited by Marc S. Dionne. *PLOS Biology* 13 (4): e1002135. https://doi.org/10.1371/journal.pbio.1002135.

Barankiewicz, Jerzy, and Amos Cohen. 1985. "Purine Nucleotide Metabolism in Resident and Activated Rat Macrophages *in Vitro*." *European Journal of Immunology* 15 (6): 627–31. https://doi.org/10.1002/eji.1830150618.

Bar-Peled, Liron, and Nora Kory. 2022. "Principles and Functions of Metabolic Compartmentalization." *Nature Metabolism* 4 (10): 1232–44. https://doi.org/10.1038/s42255-022-00645-2.

Belužić, Lucija, Ivana Grbeša, Robert Belužić, Jong Hoon Park, Hyun Kyung Kong, Nevenka Kopjar, Guadalupe Espadas, et al. 2018. "Knock-down of AHCY and Depletion of Adenosine Induces DNA Damage and Cell Cycle Arrest." *Scientific Reports* 8 (1): 14012. https://doi.org/10.1038/s41598-018-32356-8.

Bjursell, Magnus K., Henk J. Blom, Jordi Asin Cayuela, Martin L. Engvall, Nicole Lesko, Shanti Balasubramaniam, Göran Brandberg, et al. 2011. "Adenosine Kinase Deficiency Disrupts the Methionine Cycle and Causes Hypermethioninemia, Encephalopathy, and Abnormal Liver Function." *The American Journal of Human Genetics* 89 (4): 507–15. https://doi.org/10.1016/j.ajhg.2011.09.004.

Boison, Detlev. 2013. "Adenosine Kinase: Exploitation for Therapeutic Gain." Edited by Stephen P.H. Alexander. *Pharmacological Reviews* 65 (3): 906–43. https://doi.org/10.1124/pr.112.006361.

Boison, Detlev, and Michael F. Jarvis. 2021. "Adenosine Kinase: A Key Regulator of Purinergic Physiology." *Biochemical Pharmacology* 187 (May):114321. https://doi.org/10.1016/j.bcp.2020.114321.

Boison, Detlev, and Gennady G. Yegutkin. 2019. "Adenosine Metabolism: Emerging Concepts for Cancer Therapy." *Cancer Cell* 36 (6): 582–96. https://doi.org/10.1016/j.ccell.2019.10.007.

Dale, Nicholas. 2021. "Biological Insights from the Direct Measurement of Purine Release." *Biochemical Pharmacology* 187 (May):114416. https://doi.org/10.1016/j.bcp.2021.114416.

Deussen, A. 1989. "Contribution of S-Adenosylhomocysteine to Cardiac Adenosine Formation." *Journal of Molecular and Cellular Cardiology* 21 (8): 773–82. https://doi.org/10.1016/0022-2828(89)90716-5.

Dilek, Nahzli, Andreas Papapetropoulos, Tracy Toliver-Kinsky, and Csaba Szabo. 2020. "Hydrogen Sulfide: An Endogenous Regulator of the Immune System." *Pharmacological Research* 161 (November):105119. https://doi.org/10.1016/j.phrs.2020.105119.

Dolezal, Tomas. 2015. "Adenosine: A Selfish-Immunity Signal?" *Oncotarget* 6 (32): 32307–8. https://doi.org/10.18632/oncotarget.4685.

Dolezelova, Eva, Hans-Peter Nothacker, Olivier Civelli, Peter J. Bryant, and Michal Zurovec. 2007. "A Drosophila Adenosine Receptor Activates cAMP and Calcium Signaling." *Insect Biochemistry and Molecular Biology* 37 (4): 318–29. https://doi.org/10.1016/j.ibmb.2006.12.003.

Ducker, Gregory S., and Joshua D. Rabinowitz. 2017. “One-Carbon Metabolism in Health and Disease.” *Cell Metabolism* 25 (1): 27–42. https://doi.org/10.1016/j.cmet.2016.08.009.

Dulla, Chris G., and Susan A. Masino. 2013. “Physiologic and Metabolic Regulation of Adenosine: Mechanisms.” In *Adenosine*, edited by Susan Masino and Detlev Boison, 87–107. New York, NY: Springer New York. https://doi.org/10.1007/978-1-4614-3903-5_5.

Dzeja, Petras P., Susan Chung, and Andre Terzic. 2007. “Integration of Adenylate Kinase and Glycolytic and Glycogenolytic Circuits in Cellular Energetics.” In *Molecular System Bioenergetics*, edited by Valdur Saks, 1st ed., 265–301. Wiley. https://doi.org/10.1002/9783527621095.ch8.

Dzeja, Petras, and Andre Terzic. 2009. “Adenylate Kinase and AMP Signaling Networks: Metabolic Monitoring, Signal Communication and Body Energy Sensing.” *International Journal of Molecular Sciences* 10 (4): 1729–72. https://doi.org/10.3390/ijms10041729.

Fenckova, Michaela, Radka Hobizalova, Zdenek Faltynek Fric, and Tomas Dolezal. 2011. “Functional Characterization of Ecto-5′-Nucleotidases and Apyrases in Drosophila Melanogaster.” *Insect Biochemistry and Molecular Biology* 41 (12): 956–67. https://doi.org/10.1016/j.ibmb.2011.09.005.

Fleischmannova, Jana, Lucie Kucerova, Katerina Sandova, Veronika Steinbauerova, Vaclav Broz, Petr Simek, and Michal Zurovec. 2012. “Differential Response of Drosophila Cell Lines to Extracellular Adenosine.” *Insect Biochemistry and Molecular Biology* 42 (5): 321–31. https://doi.org/10.1016/j.ibmb.2012.01.002.

Fredholm, Bertil B., Stina Johansson, and Ying-Qing Wang. 2011. “Adenosine and the Regulation of Metabolism and Body Temperature.” In *Advances in Pharmacology*, 61:77–94. Elsevier. https://doi.org/10.1016/B978-0-12-385526-8.00003-5.

German, D. C., C. A. Bloch, and N. M. Kredich. 1983. “Measurements of S-Adenosylmethionine and L-Homocysteine Metabolism in Cultured Human Lymphoid Cells.” *The Journal of Biological Chemistry* 258 (18): 10997–3.

Kazek, Michalina, Lenka Chodáková, Katharina Lehr, Lukáš Strych, Pavla Nedbalová, Ellen McMullen, Adam Bajgar, et al. 2024. “Glucose and Trehalose Metabolism through the Cyclic Pentose Phosphate Pathway Shapes Pathogen Resistance and Host Protection in Drosophila.” Edited by Alex P. Gould. *PLOS Biology* 22 (5): e3002299. https://doi.org/10.1371/journal.pbio.3002299.

Klein Geltink, Ramon I, and Erika L Pearce. 2019. “The Importance of Methionine Metabolism.” *eLife* 8 (May):e47221. https://doi.org/10.7554/eLife.47221.

Kloor, Doris, and Hartmut Osswald. 2004. “S-Adenosylhomocysteine Hydrolase as a Target for Intracellular Adenosine Action.” *Trends in Pharmacological Sciences* 25 (6): 294–97. https://doi.org/10.1016/j.tips.2004.04.004.

Kornberg, Michael D. 2020. “The Immunologic Warburg Effect: Evidence and Therapeutic Opportunities in Autoimmunity.” *WIREs Systems Biology and Medicine* 12 (5): e1486. https://doi.org/10.1002/wsbm.1486.

Krejčová, Gabriela, Cecilia Morgantini, Helena Zemanová, Volker M Lauschke, Julie Kovářová, Jiří Kubásek, Pavla Nedbalová, et al. 2023. “Macrophage-derived Insulin Antagonist *ImpL2* Induces Lipoprotein Mobilization upon Bacterial Infection.” *The EMBO Journal* 42 (23): e114086. https://doi.org/10.15252/embj.2023114086.

Kroll, K, A Deussen, and I R Sweet. 1992. “Comprehensive Model of Transport and Metabolism of Adenosine and S-Adenosylhomocysteine in the Guinea Pig Heart.” *Circulation Research* 71 (3): 590–604. https://doi.org/10.1161/01.RES.71.3.590.

Latour, Yvonne L., Alain P. Gobert, and Keith T. Wilson. 2020. “The Role of Polyamines in the Regulation of Macrophage Polarization and Function.” *Amino Acids* 52 (2): 151–60. https://doi.org/10.1007/s00726-019-02719-0.

874 Lawson, Brian R., Theodoros Eleftheriadis, Virginie Tardif, Rosana Gonzalez-Quintial, Roberto Baccala,
875 Dwight H. Kono, and Argyrios N. Theofilopoulos. 2012. “Transmethylation in Immunity and
876 Autoimmunity.” *Clinical Immunology* 143 (1): 8–21. https://doi.org/10.1016/j.clim.2011.10.007.
877 Lecoq, K., I. Belloc, C. Desgranges, and B. Daignan-Fornier. 2001. “Role of Adenosine Kinase in
878 Saccharomyces Cerevisiae: Identification of the ADO1 Gene and Study of the Mutant
879 Phenotypes.” *Yeast* 18 (4): 335–42. https://doi.org/10.1002/1097-
880 0061(20010315)18:4<335::AID-YEA674>3.0.CO;2-X.
881 Lloyd, H G, A Deussen, H Wuppermann, and J Schrader. 1988. “The Transmethylation Pathway as a
882 Source for Adenosine in the Isolated Guinea-Pig Heart.” *Biochemical Journal* 252 (2): 489–94.
883 https://doi.org/10.1042/bj2520489.
884 Lu, Shelly C. 2000. “S-Adenosylmethionine.” *The International Journal of Biochemistry & Cell Biology* 32
885 (4): 391–95. https://doi.org/10.1016/S1357-2725(99)00139-9.
886 McMullen, Ellen, Lukas Strych, Lenka Chodakova, Amber Krebs, and Tomas Dolezal. 2024. “JAK/STAT
887 Mediated Insulin Resistance in Muscles Is Essential for Effective Immune Response.” *Cell*
888 *Communication and Signaling* 22 (1): 203. https://doi.org/10.1186/s12964-024-01575-0.
889 Moffatt, Barbara A., Yvonne Y. Stevens, Michael S. Allen, Jamie D. Snider, Luiz A. Pereira, Margarita I.
890 Todorova, Peter S. Summers, Elizabeth A. Weretilnyk, Luke Martin-McCaffrey, and Conrad
891 Wagner. 2002. “Adenosine Kinase Deficiency Is Associated with Developmental Abnormalities
892 and Reduced Transmethylation.” *Plant Physiology* 128 (3): 812–21.
893 https://doi.org/10.1104/pp.010880.
894 Murugan, Madhuvika, Denise Fedele, David Millner, Enmar Alharfoush, Geetasravya Vegunta, and
895 Detlev Boison. 2021. “Adenosine Kinase: An Epigenetic Modulator in Development and Disease.”
896 *Neurochemistry International* 147 (July):105054. https://doi.org/10.1016/j.neuint.2021.105054.
897 Newby, Andrew C. 1984. “Adenosine and the Concept of ‘Retaliatory Metabolites.’” *Trends in*
898 *Biochemical Sciences* 9 (2): 42–44. https://doi.org/10.1016/0968-0004(84)90176-2.
899 Novakova, Milena, and Tomas Dolezal. 2011. “Expression of Drosophila Adenosine Deaminase in
900 Immune Cells during Inflammatory Response.” Edited by Pankaj Kapahi. *PLoS ONE* 6 (3): e17741.
901 https://doi.org/10.1371/journal.pone.0017741.
902 Parkhitko, Andrey A., Richard Binari, Nannan Zhang, John M. Asara, Fabio Demontis, and Norbert
903 Perrimon. 2016. “Tissue-Specific down-Regulation of S-Adenosyl-Homocysteine via Suppression
904 of dAhcyL1/dAhcyL2 Extends Health Span and Life Span in *Drosophila*.” *Genes & Development* 30
905 (12): 1409–22. https://doi.org/10.1101/gad.282277.116.
906 Pedley, Anthony M., and Stephen J. Benkovic. 2017. “A New View into the Regulation of Purine
907 Metabolism: The Purinosome.” *Trends in Biochemical Sciences* 42 (2): 141–54.
908 https://doi.org/10.1016/j.tibs.2016.09.009.
909 Pike, M C, and C A DeMeester. 1988. “Inhibition of Phosphoinositide Metabolism in Human
910 Polymorphonuclear Leukocytes by S-Adenosylhomocysteine.” *Journal of Biological Chemistry*
911 263 (8): 3592–99. https://doi.org/10.1016/S0021-9258(18)68966-5.
912 Pike, M C, N M Kredich, and R Snyderman. 1978. “Requirement of S-Adenosyl-L-Methionine-Mediated
913 Methylation for Human Monocyte Chemotaxis.” *Proceedings of the National Academy of*
914 *Sciences* 75 (8): 3928–32. https://doi.org/10.1073/pnas.75.8.3928.
915 Reiss, Allison B., David Grossfeld, Lora J. Kasselman, Heather A. Renna, Nicholas A. Vernice, Wendy
916 Drewes, Justin Konig, Steven E. Carsons, and Joshua DeLeon. 2019. “Adenosine and the
917 Cardiovascular System.” *American Journal of Cardiovascular Drugs* 19 (5): 449–64.
918 https://doi.org/10.1007/s40256-019-00345-5.
919 Roy, Dominic G., Jocelyn Chen, Victoria Mamane, Eric H. Ma, Brejnev M. Muhire, Ryan D. Sheldon,
920 Tatiana Shorstova, et al. 2020. “Methionine Metabolism Shapes T Helper Cell Responses through

Regulation of Epigenetic Reprogramming." *Cell Metabolism* 31 (2): 250-266.e9. https://doi.org/10.1016/j.cmet.2020.01.006.

Salminen, Antero, Juha M. T. Hyttinen, and Kai Kaarniranta. 2011. "AMP-Activated Protein Kinase Inhibits NF-κB Signaling and Inflammation: Impact on Healthspan and Lifespan." *Journal of Molecular Medicine* 89 (7): 667–76. https://doi.org/10.1007/s00109-011-0748-0.

Sbodio, Juan I, Solomon H Snyder, and Bindu D Paul. 2019. "Regulators of the Transsulfuration Pathway." *British Journal of Pharmacology* 176 (4): 583–93. https://doi.org/10.1111/bph.14446.

Schädlich, Ines Sophie, Riekje Winzer, Joschi Stabernack, Eva Tolosa, Tim Magnus, and Björn Rissiek. 2023. "The Role of the ATP-Adenosine Axis in Ischemic Stroke." *Seminars in Immunopathology* 45 (3): 347–65. https://doi.org/10.1007/s00281-023-00987-3.

Shimkets, Lawrence J., and Martin Dworkin. 1981. "Excreted Adenosine Is a Cell Density Signal for the Initiation of Fruiting Body Formation in Myxococcus Xanthus." *Developmental Biology* 84 (1): 51–60. https://doi.org/10.1016/0012-1606(81)90369-9.

Singh, Sangita, Dominique Padovani, Rachel A. Leslie, Taurai Chiku, and Ruma Banerjee. 2009. "Relative Contributions of Cystathionine β-Synthase and γ-Cystathionase to H2S Biogenesis via Alternative Trans-Sulfuration Reactions." *Journal of Biological Chemistry* 284 (33): 22457–66. https://doi.org/10.1074/jbc.M109.010868.

Stenesen, Drew, Jae Myoung Suh, Jin Seo, Kweon Yu, Kyu-Sun Lee, Jong-Seok Kim, Kyung-Jin Min, and Jonathan M. Graff. 2013. "Adenosine Nucleotide Biosynthesis and AMPK Regulate Adult Life Span and Mediate the Longevity Benefit of Caloric Restriction in Flies." *Cell Metabolism* 17 (1): 101–12. https://doi.org/10.1016/j.cmet.2012.12.006.

Straub, Rainer H. 2014. "Insulin Resistance, Selfish Brain, and Selfish Immune System: An Evolutionarily Positively Selected Program Used in Chronic Inflammatory Diseases." *Arthritis Research & Therapy* 16 (S2): S4. https://doi.org/10.1186/ar4688.

Vizán, Pedro, Luciano Di Croce, and Sergi Aranda. 2021. "Functional and Pathological Roles of AHCY." *Frontiers in Cell and Developmental Biology* 9 (March):654344. https://doi.org/10.3389/fcell.2021.654344.

Xu, Yiming, Yong Wang, Siyuan Yan, Qiuhua Yang, Yaqi Zhou, Xianqiu Zeng, Zhiping Liu, et al. 2017. "Regulation of Endothelial Intracellular Adenosine via Adenosine Kinase Epigenetically Modulates Vascular Inflammation." *Nature Communications* 8 (1): 943. https://doi.org/10.1038/s41467-017-00986-7.

Xuan, Mengjuan, Xinyu Gu, Juan Li, Di Huang, Chen Xue, and Yuting He. 2023. "Polyamines: Their Significance for Maintaining Health and Contributing to Diseases." *Cell Communication and Signaling* 21 (1). https://doi.org/10.1186/s12964-023-01373-0.

Yu, Weiwei, Zhen Wang, Kailian Zhang, Zhexu Chi, Ting Xu, Danlu Jiang, Sheng Chen, et al. 2019. "One-Carbon Metabolism Supports S-Adenosylmethionine and Histone Methylation to Drive Inflammatory Macrophages." *Molecular Cell* 75 (6): 1147-1160.e5. https://doi.org/10.1016/j.molcel.2019.06.039.

Zeleznikar, R. J., R. A. Heyman, R. M. Graeff, T. F. Walseth, S. M. Dawis, E. A. Butz, and N. D. Goldberg. 1990. "Evidence for Compartmentalized Adenylate Kinase Catalysis Serving a High Energy Phosphoryl Transfer Function in Rat Skeletal Muscle." *The Journal of Biological Chemistry* 265 (1): 300–311.

Zeleznikar, Robert J., Petras P. Dzeja, and Nelson D. Goldberg. 1995. "Adenylate Kinase-Catalyzed Phosphoryl Transfer Couples ATP Utilization with Its Generation by Glycolysis in Intact Muscle." *Journal of Biological Chemistry* 270 (13): 7311–19. https://doi.org/10.1074/jbc.270.13.7311.

Zimmerman, Thomas P., Gerald Wolberg, and Gail S. Duncan. 1978. "Inhibition of Lymphocyte-Mediated Cytolysis by 3-Deazaadenosine: Evidence for a Methylation Reaction Essential to Cytolysis."

Proceedings of the National Academy of Sciences 75 (12): 6220–24. https://doi.org/10.1073/pnas.75.12.6220.